THE ANTENNA LABORATORY

RESEARCH ACTIVITIES in ---

Automatic Controls — *Antennas* — *Echo Area Studies*
Microwave Circuits — *Astronautics* — *E M Field Theory*
Terrain Investigations — *Radomes* — *Systems Analysis*
Wave Propagation — *Submillimeter Applications*

Investigations of Masers Utilizing Cross-Relaxation

by

M.H. Spring

Grant Number NsG-74-60

1093-23 15 October 1964

Prepared for:
National Aeronautics and Space Administration
1520 H Street Northwest
Washington 25, D.C.

Department of ELECTRICAL ENGINEERING

THE OHIO STATE UNIVERSITY
RESEARCH FOUNDATION
Columbus, Ohio

NOTICES

When Government drawings, specifications, or other data are used for any purpose other than in connection with a definitely related Government procurement operation, the United States Government thereby incurs no responsibility nor any obligation whatsoever, and the fact that the Government may have formulated, furnished, or in any way supplied the said drawings, specifications, or other data, is not to be regarded by implication or otherwise as in any manner licensing the holder or any other person or corporation, or conveying any rights or permission to manufacture, use, or sell any patented invention that may in any way be related thereto.

The Government has the right to reproduce, use, and distribute this report for governmental purposes in accordance with the contract under which the report was produced. To protect the proprietary interests of the contractor and to avoid jeopardy of its obligations to the Government, the report may not be released for non-governmental use such as might constitute general publication without the express prior consent of The Ohio State University Research Foundation.

Qualified requesters may obtain copies of this report from the Defense Documentation Center, Cameron Station, Alexandria, Virginia. Department of Defense contractors must be established for DDC services, or have their "need-to-know" certified by the cognizant military agency of their project or contract.

REPORT 1093-23

REPORT

by

THE OHIO STATE UNIVERSITY RESEARCH FOUNDATION
COLUMBUS, OHIO 43212

Sponsor	National Aeronautics and Space Administration 1520 H Street Northwest Washington 25, D.C.
Grant Number	NsG-74-60
Investigation of	Receiver Techniques and Detectors for Use at Millimeter and Submillimeter Wave Lengths
Subject of Report	Investigations of Masers Utilizing Cross-Relaxation
Submitted by	M.H. Spring Antenna Laboratory Department of Electrical Engineering
Date	15 October 1963

The material contained in this report is also used as a thesis submitted to the Department of Physics, The Ohio State University as partial fulfillment for the degree Maser of Science.

CONTENTS

SUMMARY

10043

The study of cross-relaxation effects in paramagnetic crystals is of great intrinsic interest to millimeter wave maser technology because of the possibility of obtaining maser amplification at higher frequency than that of the pump source. In this thesis the quantum mechanical calculation of cross relaxation rates, the rate equation analysis of the maser, and the experimental measurement of cross-relaxation rates are presented. It was shown that in materials such as ruby or emerald the cross-relaxation rate is not sufficiently strong to be practical to build a maser with its signal frequency much larger than its pump frequency. However, cross-relaxation processes could hinder or assist maser amplification in a given maser amplifier.

CHAPTER I

INTRODUCTION

The study of relaxation effects in paramagnetic crystals is carried on by many workers because of its great intrinsic interest and its importance to maser technology. Until 1958 it was thought that there were only two kinds of relaxation processes in these crystals, namely the spin-spin and spin-lattice processes characterized by the relaxation times T_2 and T_1 respectively. In 1958 Bloombergen and his coworkers[1] demonstrated that, under certain conditions, terms in the dipole-dipole interaction Hamiltonian which may be disregarded in the computation of T_2[2] may lead to a new and important relaxation effect which they called cross relaxation. This process is characterized by a relaxation time T_{21} whose magnitude, for cases where cross relaxation processes are physically important, lies in the range $T_2 \leq T_{21} < T_1$. The lower limit on T_{21} corresponds to the fact that T_2 is the fastest possible spin-spin interaction time and cross relaxation is the result of a spin-spin interaction process. The upper limit results from the fact that if $T_{21} > T_1$ the effects of cross relaxation will be masked by those of the spin-lattice relaxation.

As a simple example of a cross relaxation process let us consider the situation shown in Figure 1 where $hf_a = g_a \beta H_{DC} < hf_b = g_b \beta H_{DC}$ (g is the spectroscopic splitting factor, β is the Bohr

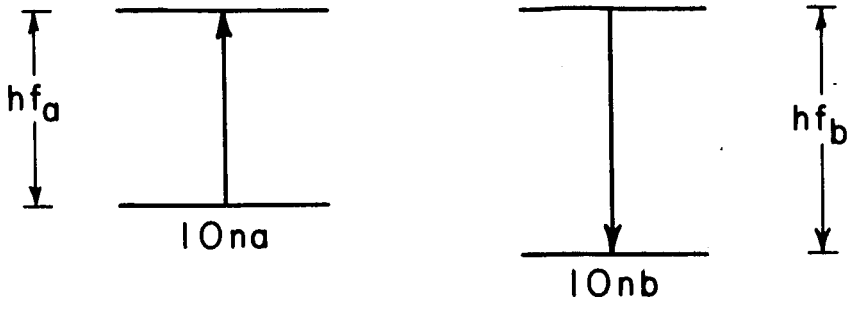

(a)

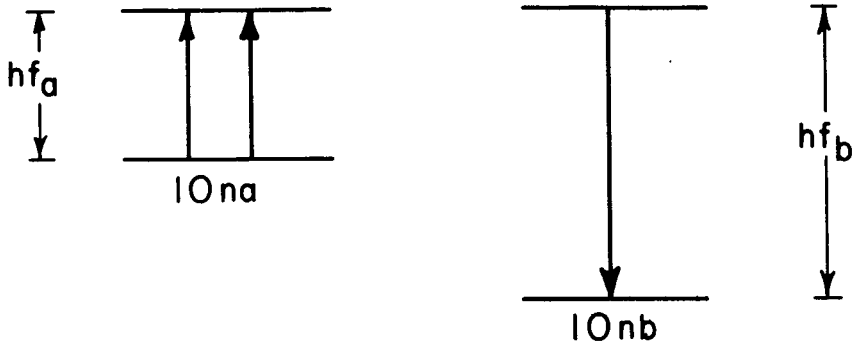

(b)

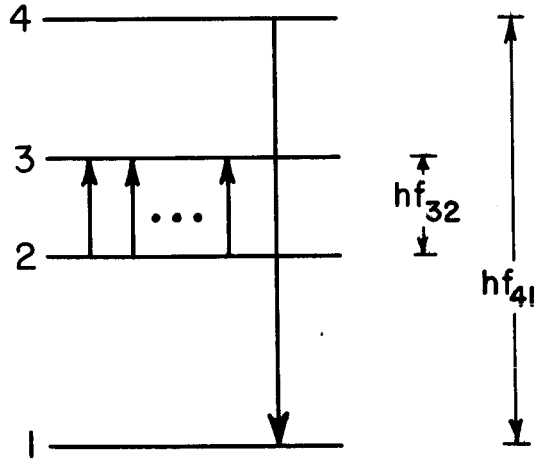

(c)

Fig. 1.

magneton and H_{DC} is the applied steady magnetic field). Such a situation could arise from two different paramagnetic ions each with spin $s = 1/2$ but with different spectroscopic splitting factors being substitutionally added into the same diamagnetic host crystal. If $f_b - f_a = f_{ab}$ is very small, i.e., if the two pairs of levels have almost the same energy spacing, a possible cross relaxation process between the a and b species is one in which one a spin makes a $\Delta m_s = +1$ transition while simultaneously a b spin makes a $\Delta m_s = -1$ transition. The excess energy hf_{ab} will be taken up by the total dipolar or internal energy of the spin system. We can write the Hamiltonian for this system as

1) $H = H_{mag} + H_{int}$

where

1a) $H_{mag} = \sum_i \beta \underline{H}_{DC} \cdot \tilde{g}_i \cdot \underline{S}_i$

is the Zeeman energy in the applied field in the general case. For our special case we have

1a') $H_{mag} = \frac{1}{2} \sum_i g_i \beta H_{DC}$.

1b) $H_{int} = \sum_{j>i} \tilde{A}_{ij} \underline{S}_i \cdot \underline{S}_j + \sum_{j>i} \tilde{B}_{ij} \left[\underline{S}_i \cdot \underline{S}_j - \frac{3(\underline{S}_i \cdot \underline{r}_{ij})(\underline{S}_j \cdot \underline{r}_{ij})}{(r_{ij})^2} \right]$

where $\tilde{A}_{ij}$ is -2 times the exchange integral, $\tilde{B}_{ij} = g_i g_j \beta^2 / r_{ij}^3$ and $\underline{r}_{ij}$ is the radius vector connecting the i-th and j-th spins.

Equation 1b can be rewritten as

$$2)\quad H_{int} = A+B+C+D+E+F$$

where

$$2a)\quad A = \sum_{j>i} A_{ij}(S_{zi}S_{zj}) \qquad A_{ij} = \tilde{A}_{ij} + \tilde{B}_{ij}(1-3\cos^2\theta_{ij})$$

$$2b)\quad B = \sum_{j>i} B_{ij}(S_{+i}S_{-j}+S_{-i}S_{+j}) \qquad B_{ij} = \tfrac{1}{2}\tilde{A}_{ij} - \tfrac{1}{4}\tilde{B}_{ij}(1-3\cos^2\theta_{ij})$$

$$2c)\quad C = \sum_{j>i} C_{ij}(S_{+i}S_{zj}+S_{zi}S_{+j}) \qquad C_{ij} = -\tfrac{3}{2}\tilde{B}_{ij}\sin\theta_{ij}\cos\theta_{ij}e^{-i\phi_{ij}}$$

$$2d)\quad D = \sum_{j>i} D_{ij}(S_{-i}S_{zj}+S_{zi}S_{-j}) \qquad D_{ij} = C_{ij}^{*}$$

$$2e)\quad E = \sum_{j>i} E_{ij}(S_{+i}S_{+j}) \qquad E_{ij} = \tfrac{3}{4}\tilde{B}_{ij}\sin^2\theta_{ij}e^{-2i\phi_{ij}}$$

$$2f)\quad F = \sum_{j>i} F_{ij}(S_{-i}S_{-j}) \qquad F_{ij} = E_{ij}^{*}$$

where S_{+1} and S_{-i} are the spin raising and lowering operators respectively and θ_{ij} and ϕ_{ij} are the polar angles of $\underline{r}_{ij}$ with respect to the coordinate axes.

If we take the usual case of $H_{mag} >> H_{int}$, we can treat H_{int} as a perturbation. The cross relaxation probability for the case under discussion is[1]

$$3)\quad W_{cr} = \hbar^{-2}\,|\langle E_i, E_j|\, H_{int}\,|E_i+hf_a, E_j-hf_b\rangle|^2 g_{ab}(f_{ab})$$

where g_{ab} (f_{ab}) is a normalized distribution function that, in essence, gives the probability that the total dipole-dipole interaction can absorb the energy hf_{ab} not accounted for by the double spin flip alone. This function, usually called the line shape function, has its maximum value when $f_{ab} = 0$. The computation of g_{ab} (f_{ab}) is discussed in chapter II.

We note that not all of the terms of H_{int} given in Equation 2 will give rise to the desired spin flip process. In fact only the B term (equation 2b) does so. This is an example of the rule that we must use only those terms given by Equation 2(or possibly combinations of those terms) in our H_{int} which give rise to the particular cross relaxation transitions of interest.

It is an interesting historical fact that the very first solid state microwave maser utilized the above type of cross relaxation process although it was not recognized as such.[3] The operation of this maser, whose active ion was gadolinium, depended upon the fact that, at the maser operating point, the frequency difference between the two energy levels of a second rare earth impurity ion in the crystal, cerium, was approximately equal to the frequency of the idler transition in the a ctive ion. Thus cross relaxation between the two transitions could take place. This gave rise to a new relaxation path for the idler transition and because $T_{21} < T_{1,cerium} < T_{1,idler}$ the effective relaxation time of the idler transition was shortened enough so that maser action could occur.

Another possible cross relaxation situation is shown in Figure 1b. Here again we have two species of paramagnetic ions but in this case we have $2f_a = f_b$. The cross relaxation process for this case will be two $\underline{a}$ spins making $\Delta m_s = +1$ transitions while one $\underline{b}$ spin makes a $\Delta m_s = 1$ transition. This is an example of harmonic cross relaxation.

For H_{int} in this case we must use combinations of the terms given in Equations 2 e.g., BC.

If, by applying a strong radio frequency signal at the frequency f_a, we saturate the f_a transition i.e., equalize the populations of the $m_s = +1/2$ and $m_s = -1/2$ levels of the a ions, it is evident that, due to the coupling of the a and b ions via the cross relaxation process, the f_b transition will tend to saturate to a degree dependent upon the strength of the cross relaxation coupling. This is an example of cross saturation which is of great importance in maser work.

As an example of this importance we note that by using ruby as the active material and excluding consideration of cross relaxation, it should be possible to make L-band (around 1400mc.) masers that operate at low magnetic fields (250-500 gauss) or at higher fields (around 2000 gauss)[4]. In practice, however, the low field maser operation is better than expected[4]. Before the discovery of cross relaxation this behavior was mysterious, after its discovery the mystery was easily cleared up. In the low field case cross saturation effects tend to minimize the population inversion of the signal transition thus reducing the maser effect; while in the high field case cross saturation acts to increase the population inversion thus enhancing the maser effect[4]. Bogle[4] has shown that, by suitable modification of the low field maser operating point, cross relaxation can be made to work to the advantage of maser operation thus making low field L-band maser operation feasible.

The energy level diagram illustrated in Figure 1c is that of an ion with a spin S = 3/2 e.g. chromium (Cr^{3+}), placed in a magnetic field whose magnitude and direction with respect to the magnetic complex axes gives rise to a splitting of the energy levels such that $mf_{32} = f_{41}$. The situation shown here may lead to the operation of a maser with a signal frequency higher than the pump frequency for if we saturate the f_{32} transition, and if the cross relaxation transition probability is large enough, the f_{41} transition will become at least partially saturated thus giving rise to the possibility of population inversion at the frequency f_{42} or at the frequency f_{31}, and each of these frequencies is larger than the pump frequency f_{32}. The essential difference between the maser operation described above and the conventional three level maser where the signal frequency is always less than the pump frequency lies in the effective multiplication of the pump frequency by the factor m through the cross saturation effect. Arams[5] has succeeded in obtaining maser action at a signal frequency of 10,590 mc. with a pump frequency of 9595 mc. using the above configuration.

It is desirable for many purposes to have a low noise continuous wave amplifier such as a maser that will operate in the millimeter wavelength region. If we have a suitable pump source there is no reason why we cannot successfully operate a conventional maser in this region. However, when we remember that for optimum results a conventional maser should have a pump frequency at least of the order of twice the signal

frequency, a glance at various manufacturers' catalogs shows that as we go higher in frequency the number of tubes that are suitable as pump sources with regard to frequency, power and, in many cases, price. This is particularly true if we want to operate a maser at a frequency above 75 Kmc. Indeed, we may find that for certain frequencies there are no commercially available sources. Thus it is desirable to be able to operate a maser using a pump source whose frequency is much lower than the desired signal frequency. We have seen that by utilizing cross relaxation it is theoretically possible to do this. The main purpose of this thesis will be to assess the feasibility of building maser devices using cross relaxation effects to obtain high signal to pump frequency ratios.

We shall discuss in Chapter II the calculation of the cross relaxation transition probability indicating the usefullness of the calculation, the difficulties involved and what we can learn from it with regard to the magnitude of T_{21} and its dependence upon the concentration of paramagnetic ions, the state functions of the energy levels involved in the process, the harmonic number m etc. Using these results, together with a rate equation analysis of the rate of change of the populations of the energy levels, we shall discuss in Chapter III the feasibility of the proposed maser device particularly with signal frequency to the pump frequency. Chapter IV will be devoted to the discussion of some experimental results relating to cross relaxation.

CHAPTER II

CALCULATION OF CROSS RELAXATION TRANSITION PROBABILITY

By way of introduction to the problem of calculating the cross relaxation transition probability w_{cr}, let us first look into the calculation of the induced absorption between two levels in a paramagnetic system. To keep things simple let us assume a system with total spin S=1/2 where the nuclear magnetic moment is zero. The spin Hamiltonian for such a system is

4) $H = g\beta \underline{H}_{DC} \cdot \underline{S} + H_{int} \qquad g\beta \underline{H}_{DC} \cdot \underline{S} >> H_{int}$

When $|H_{DC}| \neq 0$, this system will consist of two energy levels with spin quantum numbers $m_s = -1/2$ (labeled 1) for the lower level and $m_s = +1/2$ (labeled 2) for the upper level. The magnitude of the splitting is

5) $\Delta E_{21} = E_2 - E_1 = g\beta H_{DC} = hf_{21}$.

If we apply a microwave signal of frequency f_{21} to the system, the induced radiative transition rate is given by

6) $W_{12} = \frac{g^2\beta^2}{h^2} |\langle -\frac{1}{2} | H_x^{rf} S_x | +\frac{1}{2} \rangle|^2 g(f)$

where H_x is the amplitude of the applied radio frequency magnetic field whose direction is assumed to be parallel to the x-axis, and g(f) is the normalized lineshape function.

The calculation of the matrix element in W_{12} is elementary. The calculation of the lineshape function is far from elementary; in fact, no practical way has ever been found to calculate g(f) directly in any realistic case. The standard method for computing g(f) is that of the method of moments [2,6,7]. The n'th moment of g(f) is defined as

$$(7)\quad \langle f^n \rangle = \int_{-\infty}^{\infty} f^n g(f)\,df \quad \text{where} \quad \int_{-\infty}^{\infty} g(f)\,df = 1$$

A method for calculating the moments is as follows. Let $(S_x)_{nn'}$ be the matrix element connecting the single particle states n and n'. Then the normalized second moment is given by

$$(8)\quad \langle f^2 \rangle = \sum_{nn'} \left\{ f_{nn'}^2 \left| (S_x)_{nn'} \right|^2 \right\} \Big/ \sum_{nn'} \left| (S_x)_{nn'} \right|^2$$

where $f_{nn'} = (H_n - H_{n'})/h$ and H is given by Equation 4.

Van Vleck[2] pointed out that this expression can be rewritten as

$$(9)\quad h^2 \langle f^2 \rangle = -\mathrm{Tr}\left[HS_x - S_x H \right]^2 / \mathrm{Tr}\,(S_x)^2$$

where Tr stands for the trace or diagonal sum.

The process can be extended to higher moments. For instance, the fourth moment is given by

$$(10)\quad h^4 \langle f^4 \rangle = -\mathrm{Tr}\left[HU - UH \right]^2 / \mathrm{Tr}\,(S_x)^2$$

where $U = HS_x - S_x H$.

In general, the 2k'th moment is given by

$$(11)\quad h^{2K}\langle f^{2K}\rangle = (-1)^{K} \mathrm{Tr}\,[H,[H,\ldots.[H,S_x]\cdots]^2/\mathrm{Tr}(S_x)^2$$

where $[H,S_x] = HS_x - S_xH$.

Note that in the above paragraph no mention is made of the odd order moments. This is because we have made what is known as the "infinite temperature" approximation. As shown by Pryce and Stevens[8], it turns out that when we expand the moments as a function of temperature the leading terms of the even moments are independent of the temperature whereas the leading terms of the odd moments contains the factor hf/kt (k is Boltzmann's constant and T is the temperature in degrees Kelvin). As long as $hf/kt \ll 1$, which is the case throughout most of the microwave region even at $4^{\circ}K$, we may neglect the odd moments as compared to the even ones. When we are working with millimeter wavelength energy separations at helium temperatures this approximation breaks down, but we shall continue to use it on the grounds that the first moment has little effect on the line width but merely displaces the line from its room temperature position and that the whole calculation becomes even more difficult if we take the first moment into account*.

Even after this simplification we are still faced with the problem of finding a closed expression for g(f) given all the even moments.

---

* For further information on this subject see Pryce and Stevens[8] and McMillan and Opechowski[9].

This problem is complicated by the fact that, as we shall see in detail later, the difficulty in calculating the moments increases very rapidly with their order so that in practice most calculations are not carried beyond the fourth moment and, indeed, the fourth moment itself is in many cases only estimated. What is often done is to choose a Gaussian or Lorentzian lineshape and use it. The choice between them is sometimes made on the basis of computational convenience, i.e. the Gaussian shape is chosen, in the absence of other data. Of course, in some cases the lineshape function is known a priori. In other cases the goodness of fit between the experimental lineshape and the assumed lineshape can be tested by comparing the various moments. One such comparison that is commonly used is to compare the ratio of the fourth moment to the square of the second moment for both cases. Since the higher moments give progressively more information about the wings of the line and less about the center, in the absence of information about moments higher than the fourth, all we can say, even when the ratio test shows a good fit, is that we have a reasonable knowledge of the center of the line but do not know very much about what goes on in the wings.

Now let us return to the calculation. From equations 2 and 4 we have

$$(12)\quad H = g\beta H_{DC}\sum_i S_{zi} + \sum_{j>i} A_{ij} S_{zi} S_{zj} + \sum_{j>i} B_{ij}(S_{+i}S_{-j} + S_{-i}S_{+j})$$
$$+ \left\{\sum_{j>i} C_{ij}(S_{+i}S_{zj} + S_{zi}S_{+j}) + \sum_{j>i} C^{*}_{ij}(S_{-i}S_{zj} + S_{zi}S_{-j})\right.$$

$$+ \sum_{j>i} B_{ij} S_{+i} S_{+j} + \sum_{j>i} B^{*}_{ij} S_{-i} S_{-j} .$$

where we have taken the magnetic field to be in the z direction. It is clear that if we omit the terms of Equation 12 enclosed by the braces $S_z = \sum_i S_{zi}$ will commute with the remaining terms of H and hence will be a constant of the motion. Thus the selection rule for S_x, $\Delta m_s = \pm 1$ will be rigorously obeyed. The terms in the braces have selection rules $\Delta m_s = \pm 1, -2$ and when added to the first part of Equation 12 will give additional selection rules for the total Hamiltonian of $\Delta m_s = 0, \pm 2, \pm 3$ corresponding to transitions at frequencies of $f = 0$, $2g \beta H_{DC}/h$ and $3g \beta H_{DC}/h$ respectively. We are interested only in the line at $f = g \beta H_{DC}/h$ ($\Delta m_s = \pm 1$) and so we must eliminate the terms in the braces from the Hamiltonian when calculating the moments of this line since they give rise to new lines rather than to a broadening of the line of interest. The inclusion of these satellite lines in the computation of the moments would lead to erroneously large values of the moments because, even though their intensity is low, the satellite lines would count heavily in the computation due to the fact that their weighting factors, the frequency separation from the center of the line of interest, is so large. The terms of Equation 12 outside the braces constitute the truncated Hamiltonian which is to be used for this problem[2].

We note that we could have arrived at the same Hamiltonian by taking the one ion energy term, in this case the Zeeman term, and adding to it those terms of H_{int} which commute with it.

The rest of the calculation is straightforward but tedious and since we have no intrinsic interest in the spin 1/2 case we will drop it at this point*.

The extension of the above method to the case of a system with a spin $S=\frac{3}{2}$ where a crystalline electric field is present was made by Ishiguro, Kambe and Usui[10]. An example of such a system is ruby $(Cr^{3+} \text{ in } Al_2O_3)$. The one ion energy term is

13) $$H_{oi} = \beta\left[g_{\parallel} H_{DC_z} S_{z_i} + g_{\perp}(H_{DC_x} S_{x_i} + H_{DC_y} S_{y_i})\right] + D\left[S_{z_i}^2 - S(S+1)\right]$$

where $S = 3/2$.

Since in ruby $g_{\parallel} \sim g_{\perp}$ and $|D| = -D = \delta$, we can write the one ion term as

14) $$H_{oi} = -\delta\left[S_{z_i}^2 - (g\beta H_{DC}/\delta) S_{z_i}\right]$$

where we have taken the magnetic field to be parallel to the c-axis of the crystal which is also the z-axis of the magnetic complex coordinate system. We have also dropped the constant term since it does not contribute to the splitting of the energy levels.

The total Hamiltonian including interactions between the ions is

15) $$H = \sum_i H_{oi} + H_{int}.$$

---

* For further details see Van Vleck[2]

The radiative transition probability for $\Delta m_s = \pm 1$ transitions, where the microwave field is in the x direction, is given by

16) $$W_{m_s, m_s'} = \frac{g^2\beta^2}{\hbar^2} |\langle m_s | H^{rf} S_x | m_s \pm 1 \rangle|^2 g(f)$$

which is Equation 6 with an obvious modification.

The computation of the matrix element is straightforward because, due to our choice of $\underline{H}_{DC}$ parallel to the c-axis, each level is a single pure spin state. In the general case $\underline{H}_{DC}$ is not parallel to the c-axis, i.e. the polar angles θ and ϕ of $\underline{H}_{DC}$ with respect to the c-axis are not zero, and the wave function for each energy level is a mixture of pure spin states which must be calculated and hence makes the matrix element computation much more difficult.

The calculation of the second moment proceeds according to the "recipe" given in Equation 9 but as in the spin $S = 1/2$ case, and for the same reason, we must use the appropriate truncated Hamiltonian. The Hamiltonian is found by taking the one-ion energy term and adding to it those terms of H_{int} which commute with it. This turns out to be

17) $$H = \sum_i H_{0i} + \sum_{j>i} A_{ij} S_{zi} S_{zj} + \sum_{j>i} B_{ij} \left(\overline{S_{+i} S_{-j}} + \overline{S_{-i} S_{+j}} \right)$$

where

18) $$\overline{S_{+i} S_{-j}} + \overline{S_{-i} S_{+j}} = P_{3/2\,i} P_{1/2\,j} S_{+i} S_{-j} P_{1/2\,i} P_{3/2\,j} + P_{1/2\,i} P_{-1/2\,j} S_{+i} S_{-j} P_{-1/2\,i} P_{1/2\,j} + P_{-1/2\,i} P_{-3/2\,j} S_{+i} S_{-j} P_{-3/2\,i} P_{-1/2\,j} + P_{1/2\,i} P_{3/2\,j} S_{-i} S_{+j} P_{3/2\,i} P_{1/2\,j} + P_{-1/2\,i} P_{1/2\,j} S_{-i} S_{+j} P_{1/2\,i} P_{-1/2\,j}$$

$+ P_{-3/2i} P_{-1/2j} S_{-i} S_{+j} P_{-1/2i} P_{-3/2j}$

and $P_{3/2i}$, $P_{1/2i}$, $P_{-1/2i}$ and $P_{-3/2i}$ are projection operators corresponding to the states m_{si} = 3/2,1/2-1/2 and -3/2 of the i'th ion respectively.

The use of the projection operators is to ensure that we take up only $\Delta m_s = \pm 1$ transitions and in addition only those combinations of $\Delta m_s = \pm 1$ transitions which have no net effect on the total energy but merely serve to broaden the resonance line.

The above method for computing the moments of g(f) is sometimes termed the Van Vleck approach. It has the virtue of simplicity as compared to other approaches when used on the simple physical situations described above. It appears to be completely adequate in the handling of systems where no crystalline field is present or when we operate in such a manner that $\underline{H}_{DC}$ is parallel to the z-axis. The extension of this method to cases where a crystalline field is present and $\underline{H}_{DC}$ is not parallel to the z-axis is not at all obvious. The main stumbling block arises from the fact that in this case the one-ion energy term is given by Equation 13 and includes both S_x and S_y terms in addition to the S_z term. To pick out those terms of H_{int} which commute with Equation 13 is far from trivial. A much more systematic and elegant treatment is needed. Fortunately one is available, based on the work of Pryce and Stevens[8], which uses projection operator techniques throughout. This technique as used by Minkowski[11] to calculate the cross relaxation transition

rate will be discussed later on. But first, realizing the limitations of the method, it will pay us to look at the extension of the Van Vleck approach to the cross relaxation case as done by Hirone[12], who was the first to make a calculation of the cross relaxation effect in a substance having a crystalline electric field.

To illustrate Hirone's work, let us take for an example one of the systems he used, namely ruby with the one-ion spin Hamiltonian given by Equation 14 where $g\beta H_{dc}/S=1$ (see Figure 2). Let us look at the upper three energy levels. We note that

$$19)\quad hf_{32} = E_{1/2} - E_{-1/2} = 2(E_{3/2} - E_{1/2}) = 2hf_{43}$$

so that a possible cross relaxation process among these levels is one in which three ions (i,j,k), initially in the levels $m_s = 3/2$, $-1/2$, and $3/2$ respectively, make transitions so that they are finally in the levels $m_s = 1/2$, $1/2$, and $1/2$ respectively. With the setup as shown i.e. $\theta=\psi=0$, the state function for each energy level is a single pure spin state so that the above level assignments can be made unambiguously. The process described is obviously energy conserving because of Equation 19.

The probability of the indicated spin flip process is given by

$$3)\quad W_{cr} = h^{-2} |\langle \text{initial} | H_{int}(ijk) | \text{final} \rangle|^2 g(f)$$

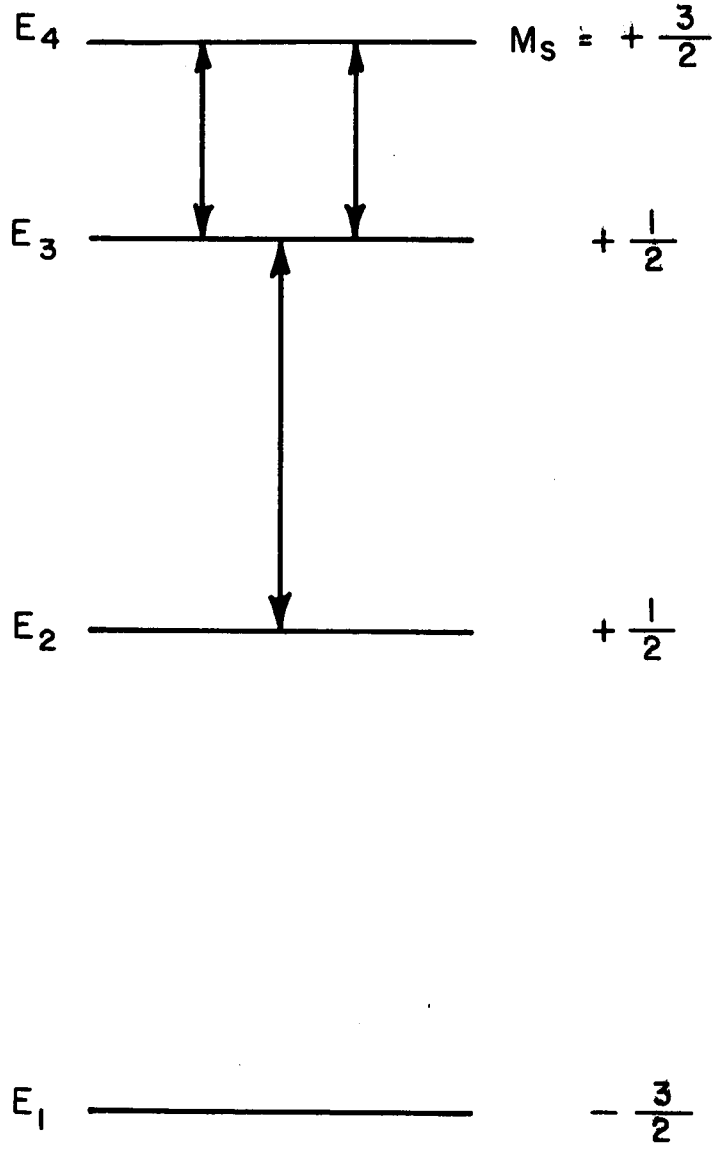

Fig. 2.

The computation of the matrix element in this case is more complicated than that in the case of the radiative transition probability because H_{int} (ijk) is a combination of terms of Equation 2 rather than just S_x. The lowest order combination of such terms of Equation 2 which gives rise to the desired process is the product of B and D with appropriate reletteringg of the subscripts. Letting n' denote an intermediate state, we have

$$20)\quad \left|H_{int}(ijk)\right|_{if} = \sum_{n'} \langle i | H'_{int}(ijk) | n' \rangle \langle n' | H''_{int}(ijk) | f \rangle / E_i - E_{n'}$$

where H_{int} (ijk) is one of the factors of H_{int} (ijk) and H''_{int}(ijk) is the other, and E_i and $E_{n'}$ are the energies of the initial and intermediate states respectively.

Equation 20 corresponds to second order perturbation theory.

Putting $h(f_{32} - 2f_{43}) = \Delta E$ and performing the sum over the intermediate states, noting that either the B or D process can occur first and that the ions i, j, and k must be near each other in order to have an appreciable interaction, we can write

$$21)\quad \langle f | H_{int}(ijk) | i \rangle = \frac{1}{\Delta E} \langle f | P_{1/2i} P_{1/2j} P_{1/2k} \{ C^*_{kj} B_{ij} (S_{-i} S_{+j} \cdot S_k S_{zj} - S_{-k} S_{zj} \cdot S_{-i} S_{+j}) + C^*_{ik} B_{ij} (S_{-i} S_{+j} \cdot S_{zi} S_{-k} - S_{zi} S_{-k} \cdot S_{-i} S_{+j}) \} P_{3/2i} P_{-1/2j} P_{3/2k} | i \rangle$$

where $P_{m_s' i}$ is the projection operator corresponding to the i'th ion being in the state $m_s = m_{s'}$.

Including the reciprocal process, we can write

$$22)\quad H_{int}(ijk) = \frac{B_{ij}}{\Delta E}\left[(C_{ik}^{\uparrow} C_{kj})\, P_{1/2i} P_{1/2j} P_{1/2K}\, S_i S_j S_{-k}\, P_{3/2i} P_{-k_2 j} P_{3/2K} + (C_{ik} - C_{kj})\, P_{3/2i} P_{-1/2j} P_{3/2K}\, S_{+i} S_{-j} S_{+k}\, P_{1/2i} P_{1/2j} P_{1/2K}\right].$$

The evaluation of the matrix element for the Hamiltonian given by Equation 22 is complicated by the fact that B_{ij} includes $\tilde{A}_{ij}$, the exchange energy, which may or may not be known, and because the terms B_{ij} etc involve sums over lattice parameters. The accuracy of the lattice sums will usually depend on the amount of computer time available*.

The method used by Horono for the calculation of the line-shape factor g(f) follows from the work of Ishiguro et al[10]. For the Hamiltonian H in the formula for the second moment given by Equation 9 we are to use the Hamiltonian given by Equation 17 which is constructed by taking the one-ion energy term and adding to it these first order terms of H_{int} which commute with it. In place of S_x we are to use H_{int} (ijk) as given in Equation 22.

Using an integral approximation to the lattice sums which assumes the exchange energy to be negligible, Hirono finds the second moment to be of the form**

---

* Hirono[12] gives a very approximate method of evaluating the lattice sums by means of an integration for the case $\tilde{A}_{ij} = 0$.

** Hirono does not actually give the form of the second term nor the value of For the case S=3/2 but we can infer both from his discussion of a similar cross relaxation process in an S=1 system.

23) $\langle f^2 \rangle = \lambda_1 (z/z-1)\, h^{-2} \overline{B_{ij}^2} + \lambda_2 \rho (z-1) \overline{B_{ij}^2}$

where λ_1 and λ_2 are numerical constants which differ by less than an order of magnitude, $\overline{B_{ij}^2}$ is an average of B_{ij}^2 (with $A_{ij}=0$) over a sphere centered at the i'th ion, z is the effective number of nearest neighbor paramagnetic ions and ρ is the concentration of such ions.* Since in most maser materials $\rho \approx 0.01$, the second term can be neglected compared to the first, thus making the second moment concentration independent.

The fourth moment may be computed from

24) $h^4 \langle f^4 \rangle = Tr\,[HU - UH]^2 / Tr\,[H_{int(ijk)}]^2$

where $U = H_{int(ijk)} H - H H_{int(ijk)}$.

Neglecting terms involving ρ, Hirono gives the fourth moment as

25) $h^4 \langle f^4 \rangle \simeq 168.48\, (z/z-1) (\overline{B_{ij}^2})^2$

Thus we have

26) $\langle f^4 \rangle \simeq 3.35\, (z-1/z)\, (\langle f^2 \rangle)^2$.

If the lineshape were Gaussian the ratio of the fourth moment to the square of the second would be exactly three. Since Hirono gets Z =8, we see that a Gaussian shape, which is

27) $g(f) = (2\pi \langle f^2 \rangle)^{-1/2} \exp\{-f^2/2\langle f^2 \rangle\}$.

is a reasonable approximation to g(f).

---

* Note that we have used a slightly different notation from that of Hirono. His B_{ij} is six times ours. In our case $\lambda_1 = 7.092$.

The above calculation suffers from the same difficulties that the calculation of Ishiguro et al[10], on which it is based, suffers from, namely grave difficulties are encountered when H_{DC} and the z-axis of the magnetic complex are not parallel. The root of these difficulties lies in the fact that in the non-parallel case the one-ion energy term contains S_x and S_y as well as S_z so that to separate out those terms of H_{int} which commute with the one-ion term becomes exceedingly difficult. In the parallel case this is easy because then the one-ion term contains only S_z. Another consideration is that in the non-parallel case, except at magnetic fields too high to be useful for maser operation, the state functions of the individual energy levels will no longer be pure spin states. Instead they will be combinations of pure spin states and the combining coefficients will be functions of H_{DC}, θ and ϕ. This situation can be included in Hirono's calculation but not without some messy notation. So if we wish to make calculations of the cross relaxation transition probability in the most general, and most common, case, the non-parallel case, we should look for a more elegant approach than that based on the work of Van Vleck. Such an approach is that of Minkowski[11] whose work is based on that of Pryce and Stevens[8]. In the following pages we shall outline Minkowski's calculation.

Neglecting interactions between ions, the total spin Hamiltonian of a system of N paramagnetic ions diluted into a diamagnetic host crystal is

28) $H_o = \sum_{i=1}^{N} H_{oi}$

where H_{oi} is the one ion energy term.

Also

29) $H_{oi} |h_i^{r_i}\rangle = \varepsilon_{r_i} |h_i^{r_i}\rangle$

where $|h_i^{r_i}\rangle$ is the r'th eigenstate of the i'th ion (referred to by Minkowski as a spin state) and ε_{r_i} is the corresponding energy. If the ion has total spin S, there are 2S +1 possible eigenstates for each ion. We also have

30) $H_o |a\rangle = E_o |a\rangle$

where $|a\rangle$ is an eigenstate of the total spin Hamiltonian (referred to by Minkowski as a system state) and E_o is the corresponding energy.

In terms of quantities associated with individual ions (spins), $|a\rangle$ has the form

31) $|a\rangle \propto \prod_{i=1}^{N} |h_i^{r_i}\rangle$

and

32) $E_o \sim n_1\varepsilon_1 + n_2\varepsilon_2 + \cdots + n_{2S+1}\varepsilon_{2S+1}$

where n_r is the population of the r'th spin state and $N = \sum_{r=1}^{2S+1} n_r$. There are

33) $N!/n_1!n_2!\cdots n_{2S+1}!$

orthogonal spin states with energy E_0.

A specific set of n_r 's, denoted by $\{n_r^\Gamma\}$ gives rise to a degenerate manifold Γ of states with an energy E_0^Γ. A projection operator on this manifold is P^Γ which can be written as the sum of projections on the states spanning the manifold.

34) $P^\Gamma = \sum_\gamma P_\gamma^\Gamma$

where γ is one of the $N!/n_1^\Gamma!\cdots n_{2S+1}^\Gamma!$ states with energy E_0^Γ.

The total spin Hamiltonian of the system, including the interaction between spins is

35) $H = H_0 + H_{int}$.

The part of H_{int} that commutes with H_0 is

36) $H_{int,c} = \sum_\Gamma P^\Gamma H_{int} P^\Gamma$

As was noted in a previous discussion, $H_{int,c}$ broadens the energy levels. Since $H_{int,c}$ and H_0 commute, they can be simultaneously diagonalized by a linear combination of "product" states of the form given in Equation 31. These states are the correct zero-order system states and are denoted by $|G\rangle$. The "product" states belonging to the manifold Γ are denoted by $|\Gamma,\gamma\rangle$. The projection operator on the Γ manifold, P^Γ, can be written as

37) $P^{\Gamma} = \sum_{G} P_{G}^{\Gamma}$

which is a sum over the correct zero-order states. Previously we wrote it as

34) $P^{\Gamma} = \sum_{\gamma} P_{\gamma}^{\Gamma}$

which is a sum over "product" states. Both forms are equally valid.

The part of H_{int} which does not commute with H_{0} is

38) $H_{int,NC} = \sum_{\Gamma} \sum_{\Lambda} P^{\Gamma} H_{int} P^{\Lambda}$

This is the part that gives rise to cross relaxation effects and will be treated as a perturbation which causes transitions between the correct zero-order states.

To first order, the energy of the Γ manifold is, using the correct zero-order system states $|G\rangle$,

39) $E_{G}^{\Gamma} = \langle G|H|G\rangle$.

In the absence of line broadening, radiative transitions will occur between two states of the manifolds $\{n_{\Gamma}^{\Gamma}\}$ and $\{n_{\Gamma}^{\Lambda}\}$ when

40) $|E_{0}^{\Gamma} - E_{0}^{\Lambda}| = hf$

where f is the frequency of the applied radiofrequency field.

Cross relaxation transitions will occur when

41) $|E_{0}^{\Gamma} - E_{0}^{\Lambda}| = 0$.

The last equation holds because, in the absence of line broadenin , cross relaxation transitions must conserve energy exactly.

When line broadening is present, the criteria become

40) $|E_G^{\Gamma} - E_L^{\wedge}| = |\langle G|H|G\rangle - \langle L|H|L\rangle| = hf$

and

41) $|E_G^{\Gamma} - E_L^{\wedge}| = \Delta E$

In the case of Equation 40 and 41 we know the lineshape is a δ function while in the case of Equations 40' and 41' it must be computed.

The cross relaxation transition probability is

42) $W_{cr} = h^{-2} |\langle G|O|L\rangle|^2 g(f)$

where O is that part of $H_{int,NC}$ which gives rise to the cross relaxation transitions of interest. If the process of interest is a three spin process such as was the case described by Hirono, O will be a three spin operator and will have the form

43) $O = \sum_{ijk\neq} O_{ijk}$

where $i \neq j \neq k$.

For an n spin process, O will obviously be an n-spin operator.

We note that the radiative transition probability is also of the form of Equation 42 except that in that case O will be a one spin operator e.g. $O_i \propto S_{x_i}$. Thus we see that both radiative and cross relaxation transitions can be treated in a uniform manner.

Since an operator such as O_{ijk} operates on the three spins k,j, and k and only on these spins, we can write

$$44)\ \langle G|\mathcal{O}|G\rangle = \sum_{ijk\neq} \langle r_i s_j t_k | O_{ijk} | r_i' s_j' t_k' \rangle$$

where $r_i s_j t_k = |h_i^r\rangle |h_j^s\rangle |h_k^t\rangle$ etc and the unprimed states are in the Γ manifold while the primed states are in the Λ manifold. The operator $\sum_{ijk\neq} O_{ijk}$ connects all permutations of $r_i\ s_j\ t_k$ to all permutations of $r_i\ s_j\ t_k$. Only some of these permutations are distinguishable e.g. we saw in discussing Hirono's work that a possible cross relaxation process resulted in all three ions winding up in the $m_s = +1/2$ state so that in the present notation r',s' and t' will be identical and hence there will be only one distinguishable permutation of the parameters. Minkowski takes account of this by rewriting Equation 44 as

$$45)\ \sum_{ijk\neq} K_{ijk} = \frac{\sigma(r's't')}{m(rst)!} |\langle r_i s_j t_k | O_{ijk} | r_i' s_j' t_k' \rangle|^2$$

where $\sigma(r's't')$ is the summation over the distinguishable permutations of r's't' and m (rst): is the number of indistinguishable permutations of rst.

We note that in general $r_i \neq r_i'$, $s_j \neq s_j'$ and $t_k = t_k'$. If we try to compute the matrix element in Equation 45 using first order perturbation theory we will always get zero for an answer since in first order theory we can write $O_{ijk} = H_{ij} + H_{jk} + H_{ik}$ where each

of the terms operates on only two spins while the state functions involve three spins so that a typical term of the computation will be

46) $\langle r_i s_j t_k | H_{ij} | r_i' s_j' t_k' \rangle = \langle r_i s_j | H_{ij} | r_i' s_j' \rangle \langle t_k | t_{k'} \rangle = 0$

since $t_k \neq t'_k$. Thus for the three spin process we must use second order perturbation theory. In general, for an m spin cross relaxation process we must use (m-1) order perturbation theory.

In the simplest three spin process, see Figure 3, $r' = s' = t'$ and $r = s \neq t$. Thus K_{ijk} becomes

47) $K_{ijk} = \frac{1}{2} K \langle r_i r_j t_k | O_{ijk} | r_i' r_j' r_k' \rangle|^2$

Following Kittel and Abrahams[13] we can convert $\sum_{ijk\neq}^{N}$, by arbitrarily choosing an origin, to

48) $\sum_{ijk\neq}^{N} = N \sum_{jk\neq}^{N} = N\rho^2 \sum_{jk\neq}^{M}$

where M is the total number of abailable sites, N is the total number of paramagnetic ions and $\rho = N/M$.

Thus for a three spin process we may write

49) $W_{cr} = \hbar^{-2} N \rho^2 \left(\sum_{jk\neq} K_{ijk}\right)(g(\Delta f))$.

with K_{ijk} defined in Equation 45.

The lineshape function is again calculated using the method of moments. The first step is to calculate the area of the line because we wishto work with normalized moments. If $|G\rangle$ and $|L\rangle$

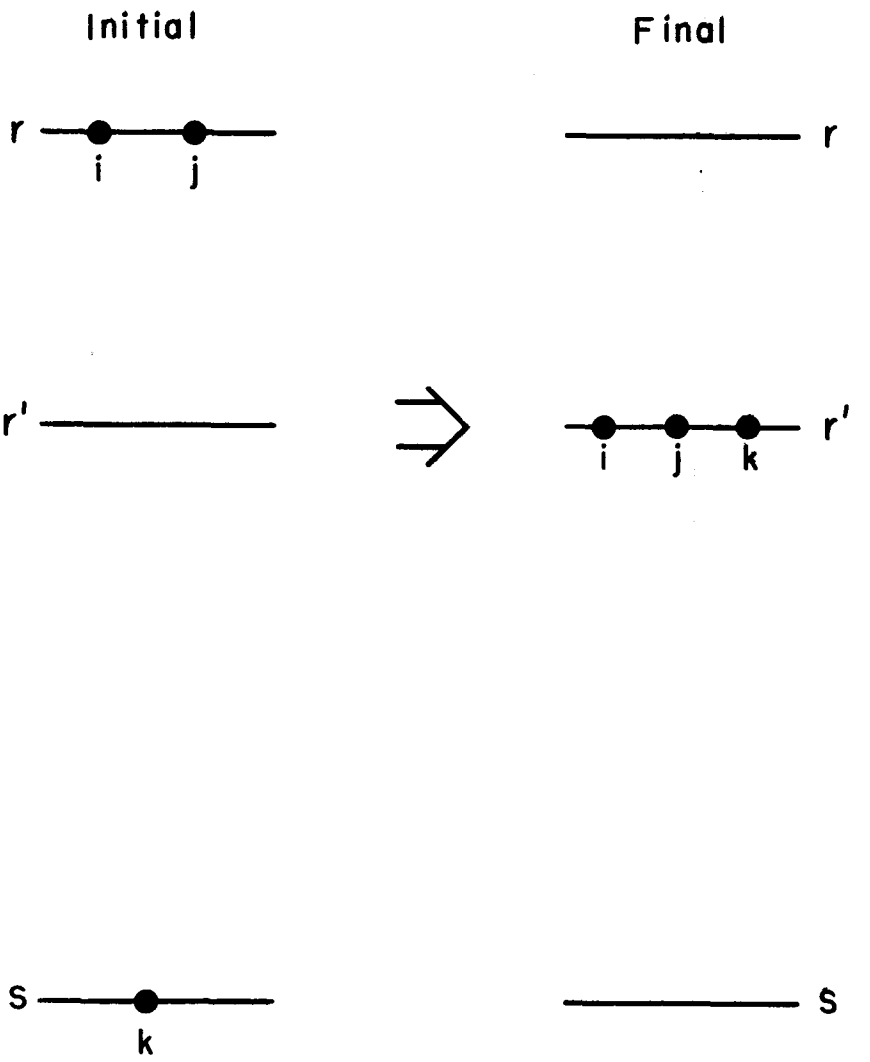

Fig. 3.

are correct zero-order system states of the manifolds Γ and Λ respectively, the area is defined as

$$50)\quad a = \sum_{\Gamma,\Lambda}\sum_{G,L} |\langle G|O|L\rangle|^2 = Tr\{OO^*\} = Tr\{O^2\}$$

which can be rewritten as

$$51)\quad a = \sum_{\Gamma,\Lambda}\sum_{G,L} \langle G|O|L\rangle\langle L|O^*|G\rangle$$

or using the projection operators P^Γ and P^Λ

$$52)\quad a = \sum_{\Gamma,\Lambda} Tr\,(P^\Gamma O P^\Lambda O^* P^\Gamma).$$

Using Equation 34 we can express the area in terms of projections over the "product" system states as

$$53)\quad a = \sum_{\Gamma,\Lambda}\sum_{\gamma}\sum_{\lambda} Tr(P^\Gamma_\gamma O P^\Lambda_\lambda O^* P^\Gamma_\gamma).$$

As before, we are interested only in transitions between distinguishable permutations i.e. physically different configurations, of the initial and final states. To this and we define the projection operator

$$54)\quad P_{ijk}^{rst} = \delta(rst)\, P_i^r P_j^s P_k^t$$

Where $\mathcal{G}(rst)$ is the sum over distinguishable permutations of rst and p_i^r is the projection operator which picks out the r'th state of the i'th ion. Thus we have

$$55)\quad \hat{O} = \sum_{i>j>k} \hat{O}_{ijk} = \sum_{i>j>k} P_{ijk}^{rst} O_{ijk} P_{ijk}^{r's't'}.$$

In converting the $\sum_{i>j>k}$ to the sum $\sum_{ijk\neq}$ we must again introduce the factor m(rst)!, the number of indistinguishable permutations of rst. Finally we have

$$56)\quad \hat{O} = \sum_{ijk\neq} \frac{\mathcal{G}(r's't')}{m(rst)!} P_i^r P_j^s P_k^t O_{ijk} P_{ijk}^{r's't'}.$$

We note that the trace in Equation 53 is to be computed in the configuration space of N spins but O_{ijk} operates only in the configuration space of three spins. Hence we can write

$$57)\quad Tr\, F(O_{ijk}) = \left(Tr^{(N-3)} I\right)\left(Tr^{(3)} F(O_{ijk})\right)$$

where $F(O_{ijk})$ is some function of O_{ijk}, the superscript over the trace operator indicates the dimensionality of the space over which the trace is to be computed and I is the identity operator. Now

$$58)\quad Tr^{(N)} I = \prod_{i=1}^{N} Tr^{(1)} I = \prod_{i=1}^{N} (2S+1) = (2S+1)^N.$$

Thus

$$59)\quad Tr^{(N)} F(O_{ijk}) = (2S+1)^{N-3}\, Tr^{(3)} F(o_{ijk})$$

Putting Equation 56 into Equation 53 and using Equations 48 and 59 we get

$$60)\quad a = (2S+1)^{N-3}\, N f^2 \sum_{j>k} K_{ijk}$$

with K_{ijk} given by Equation 45.

The unnormalized second moment for any transition line can be written as

$$61)\quad M^{(2)} = \sum_{G,L} \sum_{\Pi,\Lambda} |\langle G|H|G\rangle - \langle L|H|L\rangle|^2 |\langle G|o|L\rangle|^2$$
$$= \sum_{\Pi,\Lambda} \sum_{G,L} [\langle G|H|G\rangle\langle G|o|L\rangle - \langle G|o|L\rangle\langle L|H|L\rangle][\langle L|o^*|G\rangle\langle G|H|G\rangle$$
$$-\langle L|H|L\rangle\langle L|o^*|G\rangle]$$
$$= \sum_{\Pi,\Lambda} Tr\{(P^\Pi H P^\Pi o P^\Lambda - P^\Pi o P^\Lambda H P^\Lambda)(P^\Lambda o^* P^\Pi H P^\Pi - P^\Lambda H P^\Lambda o^* P^\Pi)\}$$

where in the last equation, the second factor is the adjoint of the first.

Since $H = \sum_{i>j} H_{ij}$, we can write

$$62)\quad P^\Lambda H P^\Lambda = \sum_\lambda \sum_{\lambda'} P^\Lambda_\lambda H P^\Lambda_{\lambda'} = \sum_{i>j} \sum_\lambda \sum_{\lambda'} P^\Lambda_\lambda H_{ij} P^\Lambda_{\lambda'}.$$

We wish to select in Equation 62 only those states $|\Lambda,\lambda\rangle$ within the Λ manifold which are connected by the terms of H_{ij}. To do this, we introduce the selection operator P_{ij}^{uv} which

operates within the Λ manifold. We can thus write

$$63)\quad \hat{H} = \sum_{i>j} \sum_{u\geq v} P_{ij}^{uv} H_{ij} P_{ij}^{uv} = \sum_{i>j} \hat{H}_{ij} .$$

Thus Equation 60 becomes

$$64)\quad M_3^{(2)} = Tr\Big\{ \Big(\sum_{i>j} \hat{H}_{ij} \sum_{k>l>m} \hat{O}_{klm} - \sum_{k>l>m} \hat{O}_{klm} \sum_{i>j} \hat{H}_{ij} \Big) \times \Big(\sum_{a>b>c} \hat{O}_{abc} \sum_{d>e} \hat{H}_{de} - \sum_{d>e} \hat{H}_{de} \sum_{a>b>c} \hat{O}_{abc} \Big) \Big\}$$

where the subscript 3 indicates a three spin process.

After taking account of all the conditions on the indices ijklm and abcde in Equation 64 which ensure that, in general, $M_3^{(2)}$ is non-vanishing (see Minkowski for the details) we get

$$65)\quad M_3^{(2)} = (2S+1)^{N-3} N p^2 \sum_{jk}^{M} G_{ijk} + (2S+1)^{N-4} N p^3 \sum_{jkl}^{M} G_{ijkl}$$

where

$$66)\quad G_{ijk} = \frac{\sigma(r's't')}{m(rst)!} |\langle rst| [H_{ij} + H_{jk} + H_{ik}, \hat{O}_{ijk}] |r's't'\rangle|^2$$

and

$$67)\quad G_{ijkl} = \sum_{u}^{M} \frac{\sigma(r's't'u)}{m(rstu)} |\langle rstu| [H_{il} + H_{jl} + H_{kl}, \hat{O}_{ijkl}] |r's't'u\rangle|^2$$

The normalized second moment is thus

$$68)\quad \langle f^2 \rangle = \frac{M_3^{(2)}}{a} = \left(\sum_{jk\neq}^{M} G_{ijk}\right) \Big/ \left(\sum_{jk\neq}^{M} K_{ijk}\right)$$
$$+ (2S+1)^{-1} \rho \left(\sum_{jkl}^{M} G_{ijkl}\right) \Big/ \left(\sum_{jk\neq}^{M} K_{ijk}\right).$$

Since in ordinary maser materials ρ is of the order of 1%, we can neglect the second term in Equation 68 compared to the first and thus we see that both Minkowski and Hirono find the normalized second moment to be concentration independent. Using a heuristic justification, which we will not go into, Minkowski finds that the leading term in all of the higher normalized moments is also concentration independent. Thus we may take f(f) to be concentration independent.

Remembering that an m-spin cross relaxation process requires (m-1)'th order perturbation theory, Minkowski approximates the area sum by

$$69)\quad \Sigma K_{ijk\ldots} \sim \rho^{(m-1)} \left(g^2\beta^2/h\bar{d}^3\right)^{2(m-1)} \left(1/\bar{f}\right)^{2(m-1)}$$

where g is the spectroscopic splitting factor, β is the Bohr magneton, $\bar{d}$ is a measure of the distance between spins (of the order of lattice dimensions) and $\bar{f}$ is an average spacing between energy levels. He similarly approximates the unnormalized second moment sum as

$$70)\quad \Sigma G_{ijk\ldots} \sim \rho^{(m-1)} (g^2\beta^2/hd^3)^{2m} (1/f)^{2(m-1)}$$

Thus the normalized second moment is given by

$$71)\quad \langle \Delta f^2 \rangle_m \sim (g^2\beta^2/hd^3)^2$$

which is independent of the order of the process. Using the values d = 4.5A and g =2 and assuming the concentration low enough so that only the concentration independent term of the second moment is significant, we find that, assuming a Gaussian lineshape, the '$e^{-1/2}$' linewidth for <u>any</u> order cross relaxation process is of the order of 550 mc.

At the center of the line, if we assume a Gaussian shape, we can approximate the cross relaxation time for an m-spin process as

$$72)\quad 1/T_{12,m} = K_{ijk}/\langle f^2 \rangle^{1/2} \sim \rho^{(m-1)} (g^2\beta^2/hd^3)^{2m-3} (1/f)^{2(m-1)}$$

Thus we have

$$73)\quad \frac{T_{12,m}}{T_{12,m+1}} \sim (\rho/f)^2 (g^2\beta^2/hd^3)^2$$

which, in the paramagnetic region, is always less than one.

That the above approximation are extremely rough ones can be seen most readily by referring to Minkowski's own experimental evidence. His energy level setup is illustrated in Figure 4. The operating point was chosen so that $f_{13} = f_{24}$ and $2f_{23} = f_{21} = f_{34}$.

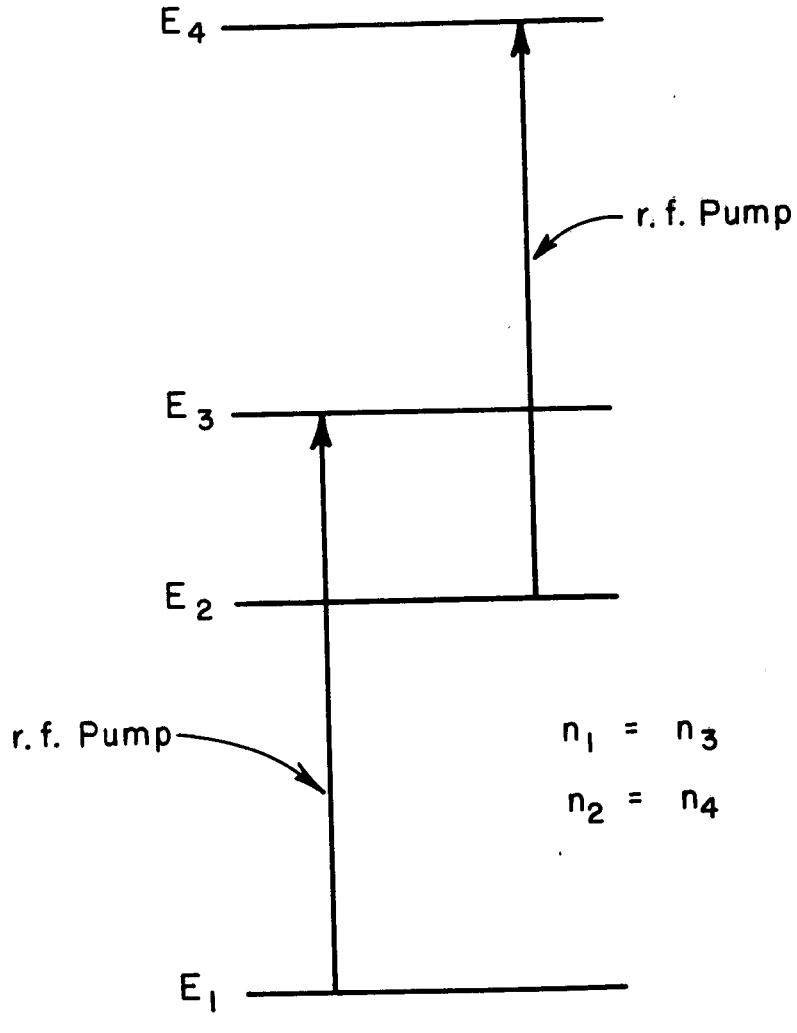

Fig. 4.

In the crystal he used, Cr^{3+} in $K_3(Co(CN)_6$, this situation occurs at $H_{DC} = 735$ gauss, $\phi = \pi/2$, and $\theta = 49°50'$. By applying a strong saturating signal at $f_{13} = f_{24}$ he was able to reduce the large number of possible cross relaxation processes to only two significant ones, $2f_{23} = f_{21}$ (the a process) and $2f_{23} = f_{34}$ (the b process). His calculation of $T_{21,a}$ and $T_{21,b}$ agreed well with his experimental results. However his results do not bear out the rough approximations made above in that the a process has a half-width of 116 mc while the b process has a half-width of 584 mc. The intensity at the center of the line of the a process is approximately three times that of the b process. Thus the approximations have only order of magnitude validity. We also see that the only essential difference between the a and b processes lies in the different state functions involved, and so we may safely assume that this is responsible for the different values of T_{21} for the two processes.

To summarize what can be learned from the quantum mechanical calculation of T_{21}, we can say that for an m-spin process the total concentration dependence, which is ρ^{m-1}, is contained in the matrix elements; that the lineshape function is, for the usual values of ρ, concentration independent; that the value of T_{21} depends critically upon the state functions of the energy levels involved in the process; and that, to within a numerical factor probably less than ten, the linewidth is independent of the order of the process. Perhaps the most important thing we have learned is that, if we know

the value of the exchange integral or, better yet, neglect it, it is possible to perform a reasonably reliable order of magnitude calculation, albeit a long and tedious one, of the cross relaxation transition probability.

CHAPTER III

RATE EQUATION ANALYSIS

In order to describe the effects of cross relaxation on the population of the various spin energy levels, we need a set of equations which include all relaxation and driving force terms. Such an equation is

$$74) \quad \frac{dn_i}{dt} = \frac{\partial n_i}{\partial t}\Big)_{S\text{-}L} + \frac{\partial n_i}{\partial t}\Big)_{rf} + \frac{\partial n_i}{\partial t}\Big)_{cr}$$

where n_i is the population of the L -th level and the subscripts S-L, rf and cr refer to spin-lattice, radiofrequency driving force and cross relaxation effects respectively.

The spin-lattice term is given by

$$75) \quad \frac{\partial n_i}{\partial t}\Big)_{S\text{-}L} = \sum_j (W_{ji} n_j - W_{ij} n_i)$$

where W_{ij} is the spin-lattice transition probability. At thermal equilibrium, if W_{ij} is the only transition causing agency present, we have

$$76) \quad N_i W_{ij} = N_j W_{ji}$$

where N_i is the thermal equilibrium population of the i-th level. In this case a Boltzmann distribution will prevail among the N_i's and thus

$$77) \quad \frac{N_j}{N_i} = e^{-hf_{ij}/KT} \qquad j > i$$

and

$$78) \quad \frac{w_{ji}}{w_{ij}} = e^{hf_{ij}/kT} \qquad j>i$$

where T is the absolute temperature of the lattice (assumed to be the same as that of the both).

Throughout this chapter we shall make use of the usual high temperature approximation $hf \ll KT$. Using this we may write

$$79) \quad N_j = N_i \left(1 - \frac{hf_{ij}}{kT}\right) \qquad j>i$$

and

$$80) \quad w_{ji} = w_{ij} \left(1 + \frac{hf_{ij}}{kT}\right) \qquad j>i$$

The approximation holds at helium temperatures throughout the centimeter wavelength region but breaks down in the millimeter region. In spite of this, and even though we are primarily interested in the millimeter region, we use the approximation because carrying through the exponentials adds little to our understanding while greatly complicating the solution of the rate equations.

The driving force term may be written as

$$80) \quad \left(\frac{\partial n_i}{\partial t}\right)_{rf} = \sum_j (n_j - n_i) W_{rf}^{ij}$$

where W_{rf}^{ij} is the radiative transition probability.

In the last chapter we computed for a three spin cross relaxation process the quantity

81) $$W_{cr} = h^{-2} N \wp^2 (\Sigma K_{ijk})\, g(\Delta f)$$

which is the cross relaxation transition probability. To see how this fits into $\left(\frac{\partial n_i}{\partial t}\right)_{cr}$ let us look at the situation shown in Figure 5 where $2f_{12} = f_{23}$. In this case W_{cr} will give us the probability that three neighboring ions will make transitions such that $n_1 \rightarrow n_1 + 2$, $n_2 \rightarrow n_2 - 3$ and $n_3 \rightarrow n_3 + 1$. To find the total number of processes per second at time t that, say, remove three ions from level 2, we must multiply W_{cr} by the probability of finding the three ions in level 2 which is $(n_2/N)^3$. The probability that there are three ions at the sites of interest is already included in Equation 81. Since each process removes three ions from level 2, the number of ions leaving level two per second at time t due to cross relaxation effects is

82) $$\left(\frac{\partial n_2}{\partial t}\right)^{-}_{cr} = 3 \frac{n_2^3}{N^2} W'_{cr}$$

where $W'_{cr} = W_{cr}/N$. Looking at the inverse process ($n_1 \rightarrow n_1 - 2$, $n_2 \rightarrow n_2 + 3$ and $n_3 \rightarrow n_3 - 1$) we readily see that

83) $$\left(\frac{\partial n_2}{\partial t}\right)^{+}_{cr} = 3 \frac{n_1^2 n_3}{N^2} W'_{cr}$$

so that the net number of ions entering level 2 is

$$84)\quad \left(\frac{\partial n_2}{\partial t}\right)_{cr} = 3\left(\frac{n_1^2 n_3 - n_2^3}{N^2}\right) w'_{cr}$$

Similarly we have

$$85)\quad \left(\frac{\partial n_1}{\partial t}\right)_{cr} = 2\left(\frac{n_2^3 - n_1^2 n_3}{N^2}\right) w'_{cr}$$

and

$$86)\quad \left(\frac{\partial n_3}{\partial t}\right)_{cr} = \left(\frac{n_2^3 - n_1^2 n_3}{N^2}\right) w'_{cr}$$

Using an obvious generalization, we see that for the case $mf_{12} = f_{23}$, which is an m + 1 spin process, we have

$$87)\quad \left(\frac{\partial n_1}{\partial t}\right)_{cr} = m\left(\frac{n_2^{m+1} - n_1^m n_3}{N^m}\right) w'_{cr}$$

where w'_{cr} must now be computed for an m+1 spin process.

Now we are ready to investigate the possibility of a harmonically pumped maser.

For a first case let us consider the energy level situation shown in Figure 6 where $mf_{23} = f_{14}$. We can write

$$88)\quad \frac{dn_1}{dt} = n_2 w_{21} + n_3 w_{31} + n_4 w_{41} - n_1(w_{12} + w_{13} + w_{14}) + \left(\frac{n_2^m n_4 - n_3^m n_1}{N^m}\right) w'_{cr}$$

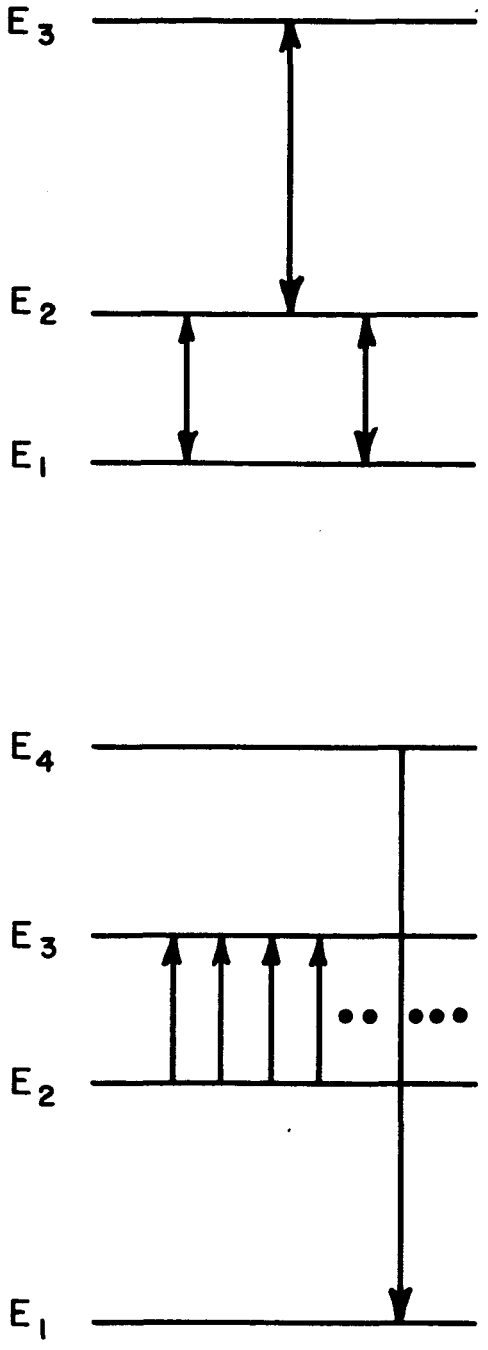

Fig. 6.

Using Equation 78, we can rewrite the above as

$$89)\quad \frac{dn_1}{dt} = w_{12}\left[n_2 - n_1 + n_2\frac{hf_{12}}{KT}\right] + w_{13}\left[n_3 - n_1 + n_3\frac{hf_{13}}{KT}\right] + w_{14}\left[n_4 - n_1 + \frac{hf_{14}}{KT}n_4\right] + \left(\frac{n_4 n_2^m - n_1 n_3^m}{N^m}\right)w'_{CT}$$

We can simplify Equation 89 as follows. In the region where $hf \ll KT$,

$$90)\quad n_i = N_i + \Delta_i$$

where $N_i \gg \Delta_i$.

Thus, for example, we have, to first order in the small quantities,

$$91)\quad \frac{hf_{12}}{KT}n_2 \approx N_2\frac{hf_{12}}{KT} = N_1\frac{hf_{12}}{KT}\left[1 - \frac{hf_{12}}{KT}\right] \approx N_1\frac{hf_{12}}{KT}$$

where we have used Equation 79. Now

$$92)\quad \sum_{i=1}^{4} n_i = \sum_{i=1}^{4} N_i = N.$$

Using Equations 71 and 92, we have

$$93)\quad N_1 = \frac{N}{4 - \frac{h}{KT}(f_{12} + f_{13} + f_{14})} \approx \frac{N}{4}$$

thus

$$94)\quad n_2\frac{hf_{12}}{KT} \approx \frac{N}{4}\frac{hf_{12}}{KT}.$$

Hence, using the high temperature approximation, we see that when the difference between two level populations is not involved we can replace n_i by $N/4$.

If we wish to use the scheme shown in Figure 6 to obtain maser action where the signal frequency is higher than the pump frequency, we will want to apply radiofrequency pump power at f_{23} so that $n_2 = n_3$. Thus letting $\Delta_{ij} = n_i - n_j$ where $j > i$, we then have, in the steady state,

$$95)\quad \frac{dn_i}{dt} = 0 = w_{12}\left[-\Delta_{12} + \frac{N}{4}\frac{hf_{12}}{KT}\right] + w_{13}\left[-\Delta_{12} + \frac{N}{4}\frac{hf_{13}}{KT}\right] + w_{14}\left[-\Delta_{14} + \frac{N}{4}\frac{hf_{14}}{KT}\right] - \Delta_{14}\left(\frac{1}{4}\right)^m w'_{cr}.$$

Letting $w''_{cr} = \left(\frac{1}{4}\right)^m w'_{cr} = \left(\frac{1}{4}\right)^m \frac{w_{cr}}{N}$, we can transform Equation 95 to

$$96)\quad \Delta_{12}\left[w_{12} + w_{13}\right] + \Delta_{14}\left[w_{14} + w''_{cr}\right] = \frac{N}{4}\frac{h}{KT}\left[w_{12}f_{12} + w_{13}f_{13} + w_{14}f_{14}\right].$$

There has not been, to the authors knowledge, any experimental or theoretical work which would enable us to evaluate reliably the various spin-lattice relaxation constants w_{ij} which appear in Equation 96. At the present stage of our knowledge, we can do little more than to hazard a guess at their relative magnitudes. We do know that, in general, $w_{ij} \neq w_{kl}$ if $i \neq k$ and $j \neq l$. In spite of this last statement, we will make the approximation that all the w_{ij}'s are equal. We do this, in the light of the fact that we cannot evaluate

the individual w_{ij}'s, in order to put the solution of the rate equations in a particularly simple form showing explicitly the dependence of the various population differences upon the physically significant parameter w''_{cr}/w_{ij}.

Making the assumption that all the w_{ij}'s are equal and denoting this value by w_{ij}, we can then write

$$97)\quad 2\Delta_{12} + \Delta_{14}\left(1 + \frac{w''_{cr}}{w_{ij}}\right) = \frac{N}{4}\frac{h}{KT}\left(f_{12} + f_{13} + f_{14}\right),$$

$$98)\quad 2\Delta_{24} + \Delta_{14}\left(1 + \frac{w''_{cr}}{w_{ij}}\right) = \frac{N}{4}\frac{h}{KT}\left(f_{14} + f_{24} + f_{34}\right)$$

and

$$99)\quad \Delta_{12} + \Delta_{24} - \Delta_{14} = 0.$$

where Equation 97 is derived from Equation 96, Equation 98 comes from transforming the equation for $\frac{dn_4}{dt}$ in the same way we transformed the equation for $\frac{dn_1}{dt}$ and Equation 99 is an identity. These three equations for a soluable set of three simultaneous linear equations from which we can extract the quantities Δ_{12}, Δ_{24} and Δ_{14}.

Solving the equation yields

$$100)\quad \frac{\Delta_{12}}{\Delta^0_{13}} = \frac{\Delta_{13}}{\Delta^0_{13}} = 1 - \frac{\left[2 + (m+1)\frac{w''_{cr}}{w_{ij}}\right]}{2\left(2 + \frac{w''_{cr}}{w_{ij}}\right)}\frac{f_{23}}{f_{13}}$$

101) $$\frac{\Delta_{24}}{\Delta^{\circ}_{24}} = \frac{\Delta_{34}}{\Delta^{\circ}_{24}} = 1 - \frac{\left[2 + (m+1)\frac{\omega''_{cr}}{\omega_{ij}}\right]}{2\left(2 + \frac{\omega''_{cr}}{\omega_{ij}}\right)} \frac{f_{23}}{f_{24}}$$

and

102) $$\frac{\Delta_{14}}{\Delta^{\circ}_{14}} \equiv \xi = \frac{2}{2 + \frac{\omega''_{cr}}{\omega_{ij}}}$$

where $\Delta^{\circ}_{ij} = N_i - N_j$; the difference of the two level populations at thermal equilibrium, and ξ is a parameter which measures the degree of saturation of the 1-4 transition due to its harmonic coupling with the externally pumped 2-3 transition.

In order to have a maser operate at the frequency f_{13}, for example, we must have $\Delta_{13}/\Delta^{\circ}_{13} < 0$. We see that, for given values of m and $\omega''_{cr}/\omega_{ij}$, the maximum rate of the signal frequency f_s $(= f_{13})$ to the applied pump frequency $f_p (= f_{23})$ will occur when $\Delta_{13} = 0$. We know that the practical maximum of the f_s/f_p ratio but, for comparitive purposes, it is useful to compute the ratio at $\Delta_{13} = 0$. Thus, for the present case, the greatest possible value of f_s/f_p is

103) $$\left.\frac{f_s}{f_p}\right)_{\Delta=0} = \frac{2 + (m+1)\frac{\omega''_{cr}}{\omega_{ij}}}{4 + 2\frac{\omega''_{cr}}{\omega_{ij}}} .$$

As a function of $\omega''_{cr}/\omega_{ij}$, $\left.\frac{f_s}{f_p}\right)_{\Delta=0}$ has its greatest value when $\omega''_{cr}/\omega_{ij} = \infty$. In this case, Equation 102 shows that $\xi = 0$ hence there is complete cross saturation. We then have

$$104) \quad \left.\frac{f_s}{f_p}\right)_{\Delta=0}^{\xi=0} = \frac{m+1}{2} .$$

We see that for finite values of $\omega''_{cr}/\omega_{ij}$ the available value of f_s/f_p is reduced from the maximum. This corresponds to incomplete cross saturation. We can see this more clearly as we rewrite Equation 103 in terms of the saturation parameter ξ thus getting

$$105) \quad \left.\frac{f_s}{f_p}\right)_{\Delta=0} = \frac{m(1-\xi)+1}{2} .$$

Thus, for a given value of m, incomplete cross saturation reduces the effective value of m and thus reduces the available f_s/f_p ratio.

Since $m \geq 1$, we see that is is theoretically possible to operate a maser using harmonic cross saturation with a signal frequency greater than the pump frequency. Naively we would say that, by making m large enough, we could get any desired f_s/f_p ratio. However, as we have seen in Chapter II, ω_{cr} is a function of the order of the cross relaxation process and, in the paramagnetic case at least, the higher the order of a spin process, the less likely it becomes. We recall from the last chapter that, putting numerical values into the admittedly rough

approximation of $\omega_{cr}(m+1)/\omega_{cr}(m)$ given in Equation 73, $\omega_{cr}(m+1)$ is at least one, and more likely two, orders of magnitude less than $\omega_{cr}(m)$. This point will be taken up later in conjunction with some experimental data.

We note that all of the above relations and comments are equally applicable to $f_s = f_{24}$. The case at hand, $mf_{23} = f_{14}$ and the pump at f_{23}, is called by Arams[5], the symmetrical case because f_s / f_p is the same for both the possible signal frequencies f_{13} and f_{24}.

What Arams[5] calls the anti-symmetric case is shown in Figure 7. Here $mf_{12} = f_{24}$ and the frequency of the pump source is f_{12}. The solution of the relevant rate equations yield

$$106)\quad \frac{\Delta_{13}}{\Delta_{13}^{0}} = 1 - \frac{\left[4+(m+2)\frac{\omega''_{cr}}{\omega_{ij}}\right]}{8+3\frac{\omega''_{cr}}{\omega_{ij}}}\frac{f_{12}}{f_{13}} = 1 - \frac{\left[2m^2(1-\xi)+m(5-\xi)+2\right]}{3(2m+1)}\frac{f_{12}}{f_{13}}$$

$$107)\quad \frac{\Delta_{34}}{\Delta_{34}^{0}} = 1 - \frac{(2m+1)\frac{\omega''_{cr}}{\omega_{ij}}}{8+3\frac{\omega''_{cr}}{\omega_{ij}}}\frac{f_{12}}{f_{34}} = 1 - \frac{\left[2m(1-\xi)+1\right]}{3}\frac{f_{12}}{f_{34}}$$

and

$$108)\quad \frac{\Delta_{24}}{\Delta_{24}^{0}} \equiv \xi = \frac{8m+4}{m\left(8+3\frac{\omega''_{cr}}{\omega_{ij}}\right)}.$$

In this case, the maximum possible f_s/f_p ratios are

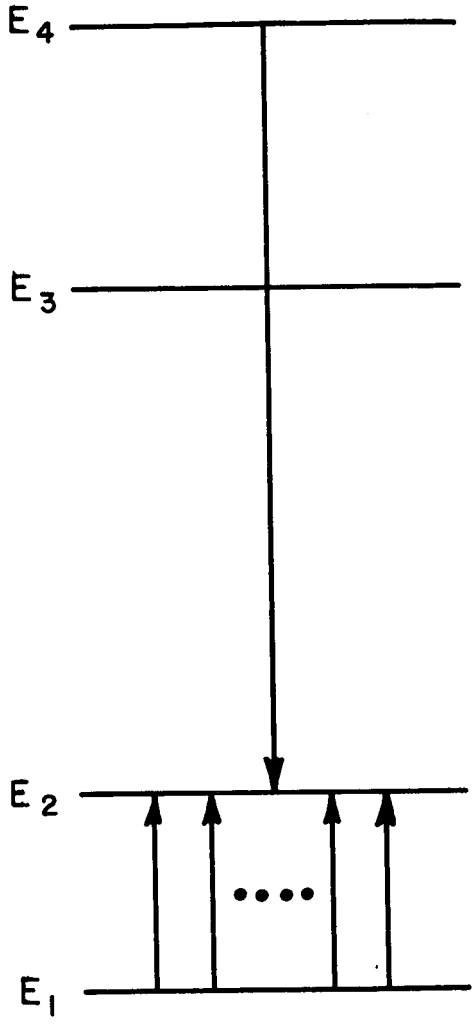

Fig. 7.

109) $$\left.\frac{f_s}{f_p}\right)_{\Delta=0}^{\xi=0} = \left.\frac{f_{13}}{f_{12}}\right)_{\Delta=0}^{\xi=0} = \frac{m+2}{3}$$

and

110) $$\left.\frac{f_s}{f_p}\right)_{\Delta=0}^{\xi=0} = \left.\frac{f_{34}}{f_{12}}\right)_{\Delta=0}^{\xi=0} = \frac{2m+1}{3} .$$

We see that using the f_{34} transition in the anti-symmetric case as our signal frequency, we can get, for the same values of m and w''_{cr}/w_{ij}, a higher value of f_s/f_p than for either of the possible signal frequencies in the symmetric case.

If we wish to operate a maser using either of the schemes just discussed, or for that matter any maser, we must make sure that there are no interfering cross relaxation process in the region of interest. As an example of the effects of interfering processes, consider the symmetric case where we have the additional cross relaxation process $pf_{12} = f_{24}$. This will add the (linearized) term $w''_{cr}(p)\times[-p\Delta_{12}+\Delta_{24}]$ to the rate equations. Thus the interfering process tends to make both Δ_{12} and Δ_{24} approach zero. When we recall that

for the symmetric case $\Delta_{23}=0$ and $\Delta_{14}\to 0$, we see that the net effect of the $pf_{12}=f_{24}$ process is to make all of the various population differences approach or equal to zero. The only way out of this difficulty is to choose an operating such that all potentially interfering processes are either absent or of very low intensity. Recalling the statement that cross relaxation processes are significant only in the region where $T_2 \leq T_{21} < T_1$, we see that we can, quantitatively, ignore all those interfering processes whose magnitude satisfies the condition $\frac{T_1}{T_{21}} = \frac{W_{cr}}{W_{ij}} < 1$ because in these cases the effects of spin-lattice relaxation will be the dominant effects. The above inequality is called the isolation condition by Bicknell[14]. It is more stringent than appears at first glance because of the finite linewidth of cross relaxation processes. Thus processes which, at our operating point, are non-energy conserving up to around 1 Kmc may possibly not satisfy the isolation condition. It is thus possible that in a crystal which has many potential operating points suitable from the standpoints of signal frequency, f_s/f_p ratio, W'_{cr}/W_{ij} ratio etc., there may well be only a few, one or even none that are suitable when interfering cross relaxation processes are taken into account. A similar statement holds for conventional three level masers. However, as shown in Equation 105, for a given crystal and a given transition whether a maser with f_s much greater than f_p can

be made depends critically upon the saturation parameter. For this reason and because of the lack of any existing data on ω_{ij} and ω_{cr} an experimental investigation was carried out for the measurement of cross saturation effects in ruby. This investigation is described in the next chapter. Obviously what is true with respect to ruby does not necessarily apply to other crystals but the experimental data will give us an idea of what values of ξ can be expected.

CHAPTER IV

EXPERIMENTAL INVESTIGATION

In order to gain some idea of the possibility of building a millimeter maser device utilizing harmonic cross saturation, we attempted to measure the effect in ruby at centimeter wavelengths. Among the reasons for using ruby are that it is easily obtainable, its energy levels are well known and that the results obtained will also be characteristic of emerald, a material suitable for millimeter wavelength masers, which is quite similar to ruby except for having a zero field splitting of 53.6 Kmc. which is 4.66 times the 11.5 Kmc. splitting of ruby. The operational frequency range was dictated by the availibility of the components.

The first step in the experimental process is to choose the lower pump frequency and then to construct a transition map showing the pump frequency and its first few harmonics as a function of H_{DC} and θ, the angle between H_{DC} and the c-axis of the crystal. A portion of such a map is shown in Figure 8. The intersections of the harmonic transition curves with the pump transition curve serves to locate the various possible operating points at which we can measure the cross saturation effect using our apparatus.

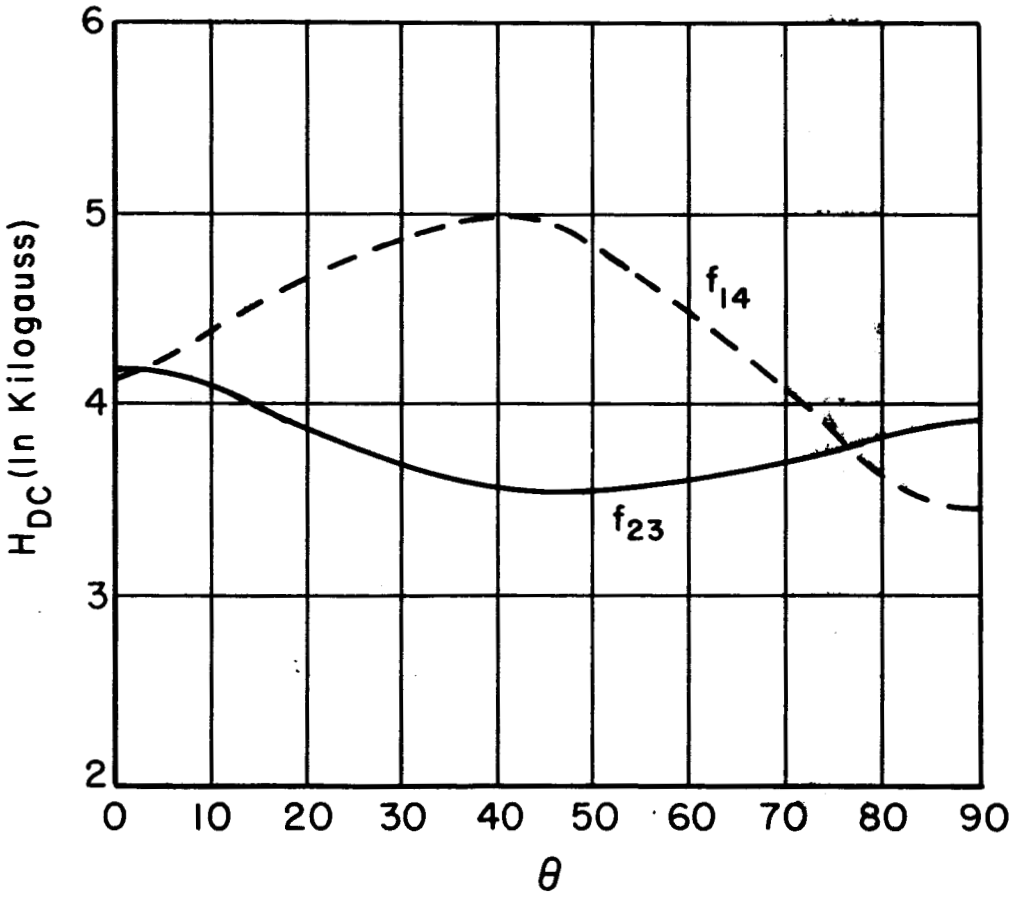

Fig. 8.

Figure 9 shows a schematic diagram of the experimental setup. We see that the setup consists essentially of two simple crystal video paramagnetic resonance spectrometers, one at X-band, 11-12 Kmc, with provision for harmonic mixing of the two signals so as to enable us to compare the frequency of the V-band signal to the frequency of the third harmonic of the X-band signal. For our harmonic mixer we used a standard X-band crystal and mount and this combination gave excellent results. The microwave cavity is illustrated in Figure 10. With no dielectric material inside the cavity, the dimensions of the cavity are such that it is above cutoff for V-band and beyond cutoff for X-band. With the dielectric spacer and the ruby disk in place, flush against the top of the cavity, X-band above cutoff propagation is allowed within the volume occupied by the dielectric-ruby cylinder while only evanescent modes will be found outside this region. Thus, unless the moveable plunger, which tunes the V-band resonance frequency, is extremely close to the dielectric, there will be no change in the X-band cavity resonance frequency while the V-band cavity resonance frequency is being changed. The X-band cavity resonance frequency is fixed by the dimensions and the dielectric constant of the dielectric-ruby cylinder and is therefore not tuneable. This latter is no hardship since all we need at X-band is one well defined reasonably high Q cavity resonance somewhere between 11 and 12 Kmc. In practice we can always get at least one such resonance by, if necessary, changing the height of the dielectric spacer.

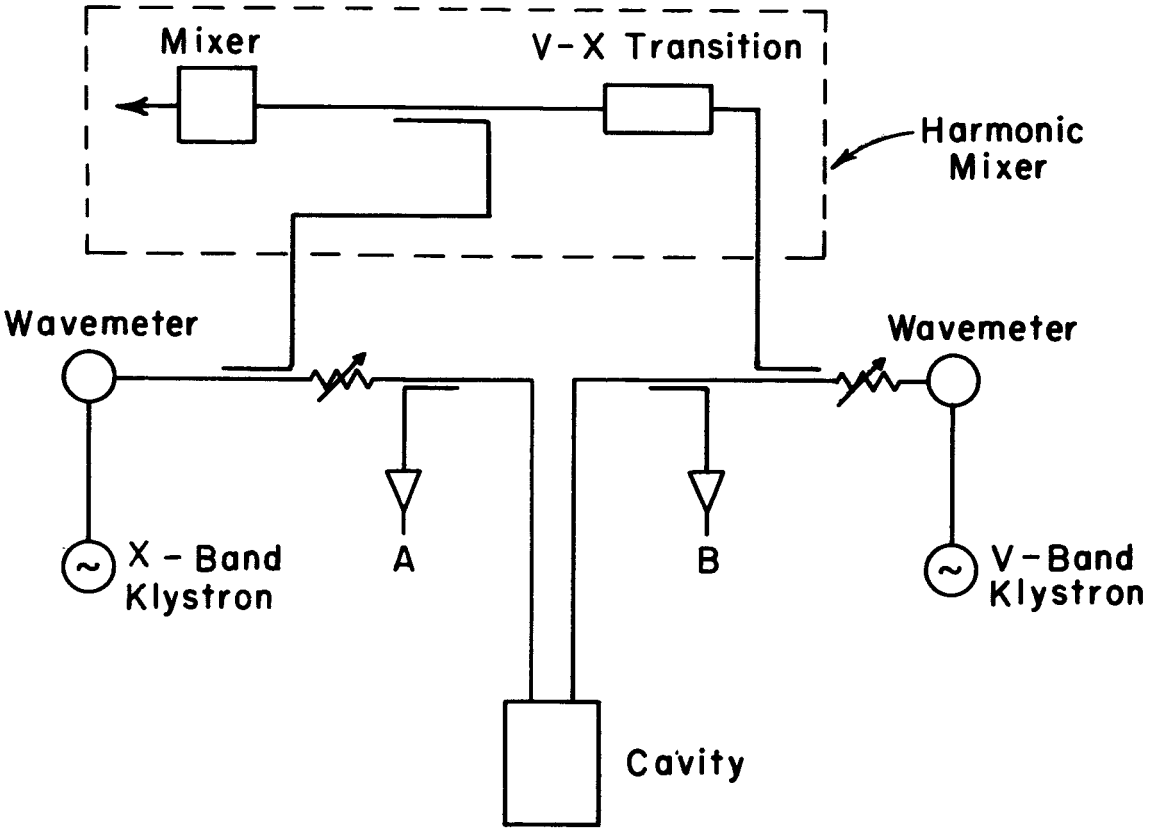
Mixer
V-X Transition
Harmonic
Mixer
Wavemeter
Wavemeter
X - Band
Klystron
A
B
V-Band
Klystron
Cavity

Fig. 9.

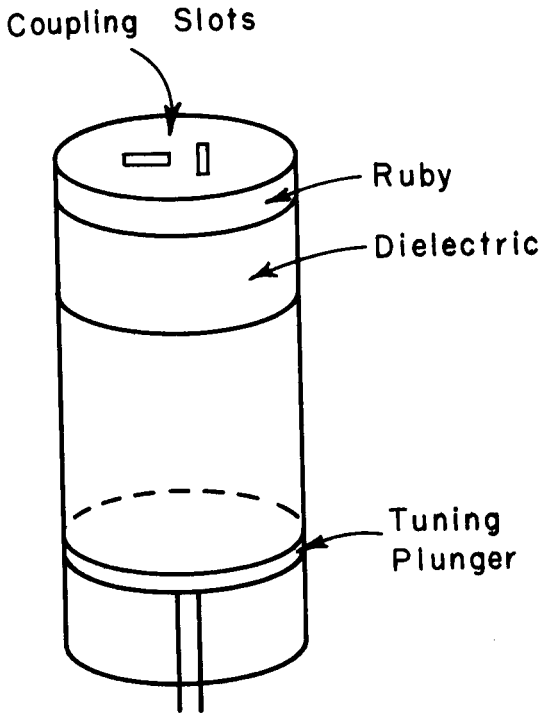

Fig. 10.

The measurement procedure is as follows. We first set the X-band frequency, with the klystron in the c.w. mode, to the center of the X-band cavity resonance. Then with both klystrons in the c.w. mode, we feed some X-band and V-band signal power into the harmonic mixer, tune the V-band frequency until we get a zero-beat with the third harmonic of the X-band frequency and tune the V-band wavemeter to this frequency and the X-band wavemeter to the X-band frequency. We then switch both klystrons to the f.m. mode and, using the wavemeter pips as markers, center both cavity resonances in the respective klystron modes. Now the magnetic field is adjusted so that we can see simultaneous X-band and V-band paramagnetic resonance on our oscilliscope (s) at the desired operating point. A dual beam oscilliscope is highly desireable for this work although it is possible to use two single beam oscilliscopes. Next, with the magnetic field off the paramagnetic resonance point, we read off the distance $Q = Q_{off\text{-}res}$ for both cavity dips, making sure that we have moved both wavemeter pips out of the picture. (see Figure 11a) Then we must measure the height b which is the height of the mode at the desired operating frequency in the absence of a cavity resonance at that frequency. In the case of the X-band, we do this by placing the wavemeter pip at a convenient point on the shoulder of the mode, (see Figure 11b), shorting the waveguide as close to the top of the dewar as possible, adding enough attenuation to the line to bring the

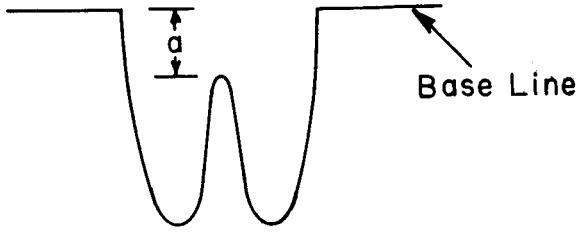

(a)

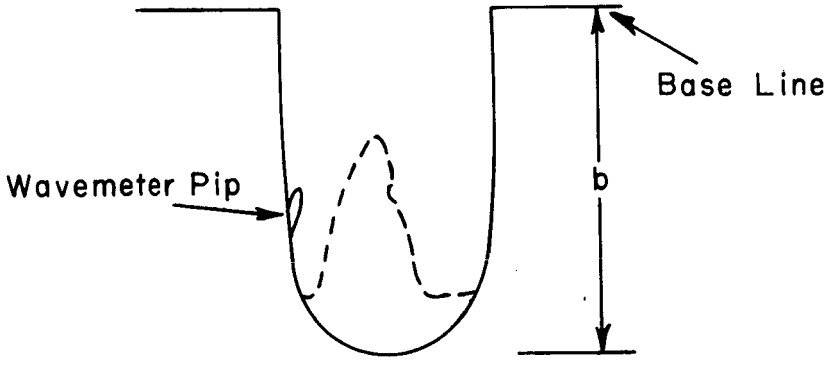

(b)

Fig. 10a and b.

marker pip back to its original and then measuring the distance b (figure 10b). Then return the apparatus to the previous state. Normally, all that has to be done to measure b for the V-band mode is to move the tuning plunger so that no cavity resonance can be seen anywhere on the cavity mode. Sometimes, due to the fact that the V-band cavity is highly multi-moded and hence there will be many resonances close together, the above procedure is not feasible and then we measure b in the same way as we do in the X-band case. From these two pieces of data, $a_{off\text{-}res}$ and b, we can compute, in the manner shown below, β_0, the cavity coupling coefficient in the absence of paramagnetic resonance *.

Then, reestablishing the condition of paramagnetic resonance and keeping the V-band power level low enough so as to cause no self-saturation of the V-band transition (it must be the same power level at which we measured the a and b described above) and the X-band power level at the detector constant by means of a compensating attenuator in front of the X-band detector, we proceed to measure a_x and a_v as a function of X-band power starting at a low enough X-band power level so that no self-saturation of the X-band transition is discernable in the first measurement. This is called the unsaturated measurement. We continue the measurements until the X-band

---

* This assumes that the length of waveguide between the top of the dewar and the cavity itself can be neglected, which it can be.

transition is completely self-saturated or an increase in X-band power causes no further increase in the V-band cross saturation, whichever comes first. We then return to the initial conditions and start in again making measurements only this time we change the V-band frequency to $f_{V_1} = 3f_x + \Delta_1$, where Δ_1 is the smallest convenient frequency change we can make. After these measurements we shift to a frequency increment Δ_2 where $|\Delta_2| > |\Delta_1|$, then to an increment $|\Delta_3| > |\Delta_2|$ etc. We should continue to make measurements out to values of Δ of the order of $\pm$ 400 mc or so or until the value of a_V with the X-band transition completely saturated becomes stationary or begins to decrease. In this way we can find the rough lineshape of the process, since over these small changes in H_{DC} and θ we can take ω_{ij} to be constant; the value of ω_{cr}/ω_{ij}; the degree of cross saturation due to spin-lattice effects alone, since in the far wings $\omega_{cr} \approx 0$; and hence something about the value of ω_{cr} itself. Ideally, those are the things we should find out by putting the data into the computation method described below. In practice, various problems arose in our particular experiment which prevented us from getting good quantitative data concerning ω_{cr} (or ξ). These problems are discussed immediately following the computation method.

Computation Method

For any microwave cavity we have

111) $$\frac{1}{Q_o} = \frac{1}{Q_c} + \frac{1}{Q_m}$$

where Q_o is the total unloaded Q of the cavity, Q_c is the unloaded Q of the cavity in the absence of paramagnetic resonance absorption and includes the ohmic losses due to the finite conductivity of the walls and of the dielectric media inside the cavity etc. and Q_m is the magnetic Q which takes into account only the losses due to paramagnetic resonance absorption. We can rewrite Equation 111 as

112) $$Q_o = Q_c Q_m / Q_c + Q_m .$$

The cavity coupling coefficient, β , can be written as, in all but a few very unusual cases which we need not consider here,

113) $$\beta = Q_o / Q_{ext}$$

where Q_{ext} is external Q of the cavity system. Combining Equations 112 and 113 gives

114) $$\beta = (Q_c Q_m / Q_c + Q_m)(1 / Q_{ext}) .$$

In the absence of paramagnetic resonance we have

115) $$\beta_o = Q_c / Q_{ext} .$$

Thus

116) $$\frac{\beta}{\beta_o} = \frac{Q_m}{Q_c + Q_m}$$

or

117) $$Q_m = Q_c \, (\beta/\beta_o)/(1 - \beta/\beta_o)$$

Denoting by the subscript u the case where paramagnetic resonance absorption is present but there is no saturation of the transition whatsoever, and by the subscript s the case where there is evidence of saturation, we have

$$118) \quad \frac{Q_{m_s}}{Q_{m_u}} = \left(\frac{\beta_0 - \beta_s}{\beta_s}\right)\left(\frac{\beta_u}{\beta_0 - \beta_u}\right)$$

The magnetic Q of a transition is proportional to the population difference between the levels involved in the transition. In the completely unsaturated case, the population difference involved is just the thermal equilibrium population difference, Δ^0_{ij}, (using the notation introduced in Chapter III), and in the saturated case is denoted by Δ_{ij}. Thus we get

$$119) \quad \frac{Q_{m_s}}{Q_{m_u}} = \frac{\Delta_{ij}}{\Delta^0_{ij}} \equiv \xi = \left(\frac{\beta_0 - \beta_s}{\beta_s}\right)\left(\frac{\beta_u}{\beta_0 - \beta_u}\right)$$

where ξ is the saturation parameter also introduced in Chapter III. Now

$$120) \quad \beta = \frac{1 - |\Gamma|}{1 + |\Gamma|}$$

where Γ is the reflection coefficient measured at the cavity terminal in the case that the cavity is undercoupled. Since these terminals are not accessible, we use an indirect method of measuring $|\Gamma|$. The power incident on either one of the detectors in the setup is

121) $P_{Det} = P_{KlYS}\, \alpha_1 \alpha_2 |\Gamma|^2$

where P_{KlYS} is the power output of the klystron tube, α_1 is an attenuation factor which includes all the losses in the microwave line between the klystron and the cavity and α_2 includes all losses between the cavity and the detector. Off resonance, a microwave cavity of the type we have here acts as a short circuit terminating the line. In this case $|\Gamma_{off\text{-}res}|^2 = 1$. If we keep the power level incident on the crystal detector low enough, we can assume square law detection i.e., the output voltage is proportional to the incident power. We remember that distances measured on the oscilloscope screen are actually voltages. Hence

122) $|\Gamma|^2 = \frac{a}{b}$

since the attenuation factors are constants and we take care to keep P_{KLYS} constant. Thus we see that, using the experimentally measured quantities a and b, it is a relatively simple matter to calculate ρ_Γ and hence, using the results of chapter III, ω_{cr}/ω_{ij}. The accuracy of the final result may not be too great even if the experimental conditions are perfect because the closer the transition comes to being completely saturated, the closer β_s approaches β_o and Equation 118 shows that we are then subtracting two nearly equal quantities neither of which is known to great precision because of the difficulty in getting readings of more than two significant figures from an

oscillocope. It would have been better to use a c.w. system rather than the f.m. system we did use thus enabling us to utilize a more precise readout system such as a meter or a chart recorder, but, because of the time and expense involved, it was felt that to build the necessary a.f.c. systems for the c.w. setup would be foolish as there would be no further use for them once this project was completed.

Much more serious problems arose which made the accuracy of the calculation a moot point. One was the non-repeatability of the quantitative data. It was possible on only a very few experimental runs for us to be able to take a set of data at a particular frequency and to then immediately take another set of data at the same frequency and to have the two sets of data agree to within a few per cent. A convenient checkpoint to use for checking the compatibility of two sets of data is the value of a when the magnetic field is off para-magnetic resonance. This value changed from run to run. It was also noticed that during the application of a large amount of X-band pump power, such as is necessary to ensure complete saturation of the X-band transition, the problem was aggravated by a change in the V-band cavity resonance frequency. This change in cavity frequency naturally precluded any measurements.

The shifting of a from run to run was never cleared up but, although it was a serious handicap, it did not make the experiment impossible because there were times when this shift did not occur.

A plausible explanation for the shift of the V-band resonance frequency with X-band power is that the X-band power boiled off the helium inside the cavity. The peak power available from our tube, an X-13 klystron, was of the order of 90mw. and of this about 30mw or so was the maximum power into the cavity and this is sufficient to cause boiling. Such power was needed because of the size of the sample which was in turn necessitated by the lack of sensitivity of the V-band spectrometer. In an effort to curve the problem we tried operating below the lambda point of the helium but to no avail. We also tried to keep liquid helium out of the cavity. Since the cavity could not be sealed off due to the hole necessary for the plunger shaft in the bottom wall of the cavity, we did this by turning the X-band power up to maximum and keeping it there until no further change in the V-band resonance frequency was observed and then on a heater element, which was a resistor, located in the space between the bottom side of the plunger and the bottom side of the cavity. Since the ruby was in direct contact with the cavity walls which in turn were in direct contact with the liquid helium, there should have been no great rise in the temperature of the sample particularly as the heater power was kept at the minimum level which would keep the V-band resonance constant in frequency. This technique was only partially successful but it did enable us to get one piece of quantitative data.

Our data was taken on the three spin cross relaxation process $2f_{12} = f_{24}$. There we found that the maximum degree of cross saturation was about $\xi_{24} = .11$. This corresponds to, making us of Equation 108, $w_{cr}/w_{ij} = 27.6$ and to a maximum fs/fp ratio of, using Equation 107, $\left(\frac{f_s}{f_p}\right)_{\Delta=0} = \left(\frac{f_{34}}{f_{12}}\right)_{\Delta=0} = 1.5$. These figures should not be taken too literally but they are in the same ballpark with figures from other workers and tend to cast doubt upon the possibility of obtaining fs/fp ratios significantly higher than one.

Bicknell[14] examined the case of $3f_{34} = f_{13}$ in .05% ruby at 4.2°K and found no inversion whatsoever, but does not give a value for ξ. He measured ξ for the process $3f_{23} = f_{14}$ in the same crystal and got $\xi = .06$ but he did not look for any inversion because of his use of the criterion that a useful situation for maser action must have $\frac{w_{cr}}{w_{ij}} \geq 200$ which is equivalent to saying that, allowing for his claimed 1% experimental error, ξ must be $\leq .01$ experimentally or theoretically, zero. With $\xi = 0$ there is, of course, no diminuation of the fs/fp ratio and this is his reason for using the criterion. In any event, $\xi = .06$ would yield $\left(\frac{f_s}{f_p}\right)_{\Delta=0} = 1.9$ and $\frac{w_{cr}}{w_{ij}} \approx 31$. This was the smallest value of ξ for any four spin process he measured.

Mims and McGee[15] found that T_{21} for various m = 2 processes in .1% ruby ranged from .2 to 1.3 x 10^{-3} sec. with most of the order of 1 x 10^{-3} sec. They also found that at 4.2°K, $T_1 \approx .1\ C^{-1}$ m sec. Assuming that Pace et al[16] are correct, $T_1 \propto 1/T$ and thus at 1.5°K,

$T_1 \approx 280^{-1}$ m sec. For a .1% concentration $T_1 = 280 \times 10^{-3}$ sec. Thus $\frac{T_1}{T_{21}} = \frac{W_{cr}}{W_{ij}} \approx$ 280 for m = 2 processes in .1% ruby at 1.5°K.

Increading the concentration of the paramagnetic ion will increase the value of W_{cr} but there is an upper limit to the useable concentration. This limit is given by the concentration at which strong cross relaxation effects are observed between all pairs of transitions irrespective of the energy imbalance. Experimentally it is observed that, in ruby, such a general cross relaxation effect occurs at concentrations above 0.15%[14,15].

When we remember that in an m + 1 spin process is less likely than an m spin process by at least an order of magnitude, we readily see that masers with value of fs/fp much greater than one are not possible in ruby at least nor do they seem very feasible in other substances unless one can find a substance which has an extremely long spin-lattice relaxation time, at least an order of magnitude or, better yet, two greater than that of ruby, with a comparable cross relaxation time. Thus, at the present time, it would seem that greatest use of cross relaxation in maser devices at millimeter as well as at all other wavelengths will be to aid in the performance of conventionally pumped masers.

REFERENCES

1. Bloembergen, N., Shapiro, S., Pershan, P.S. and Artman, J.O., Phys. Rev., 114, 445 (1959)
2. Van Vleck, J.H., Phys. Rev., 74, 1168 (1948)
3. Feher, G. and Scovil, H.E.D., Phys. Rev., 105 760, (1957)
4. Bogle, G.S., Proc. IRE, 49, 573, (1961)
5. Arams, F., Trans. IRE, MTT-9, 68, (1961)
6. Waller, I., Zeits. f. Physik, 79, 380, (1932)
7. Broer, L.J.F., Physica, 10, 801, (1943)
8. Pryce, M.H., and Stevens, K.W., Proc. Phys. Soc. (London), A63, 36, (1950)
9. McMillan, and Opechowski, Canad. J. Phys., 38, 1168, (1960); 39, 1369, (1961)
10. Ishigvro, E., Kambe, K., and Vsui, T., Physica, 17, 310, (1951)
11. Minkowski, J.M., "Cross Relaxation on Non-Zeeman Spin Systems," Tech. Rep. AF-101, The Johns Hopkins University, Carlyle Barton Lab., Baltimore, Md., Feb. 1963.
12. Hirono, M., J. Phys. Soc. Japan, 16, 766, (1961); 17, 788 (1962)
13. Abraham, E. and Kittel, C., Phys. Rev., 90, 238, (1953)
14. Bicknell, W.E., "An Attempt at 3:1 Harmonic Pumping of a Ruby Maser," Tech. Rep. 0554-1, Electron Devices Lab., Stanford Univ., Stanford, California, Oct. 1963.

References Continued

15. Mims, W. and McGee, J., Phys. Rev., 119, 1233, (1960)

16. Pace, J.H., Sampson, D.F., and Thorp, J.S., Proc. Phys. Soc. (London), A76, 697, (1960).